SURFACE DEPLETION CORRECTION TO CARRIER PROFILES BY
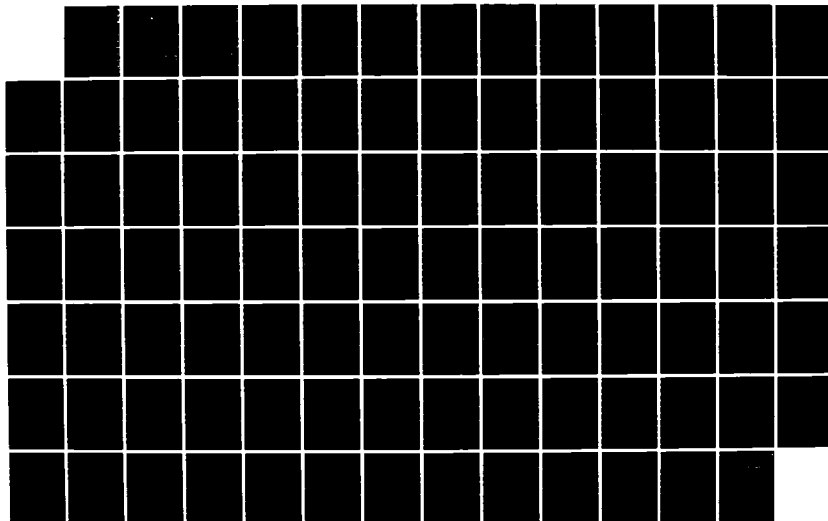HALL MEASUREMENTS(U) AIR FORCE INST OF TECH
WRIGHT-PATTERSON AFB OH SCHOOL OF ENGINEERING

D W ELSAESSER DEC 85 AFIT/GEP/ENG/85D-3   F/G 20/12   NL
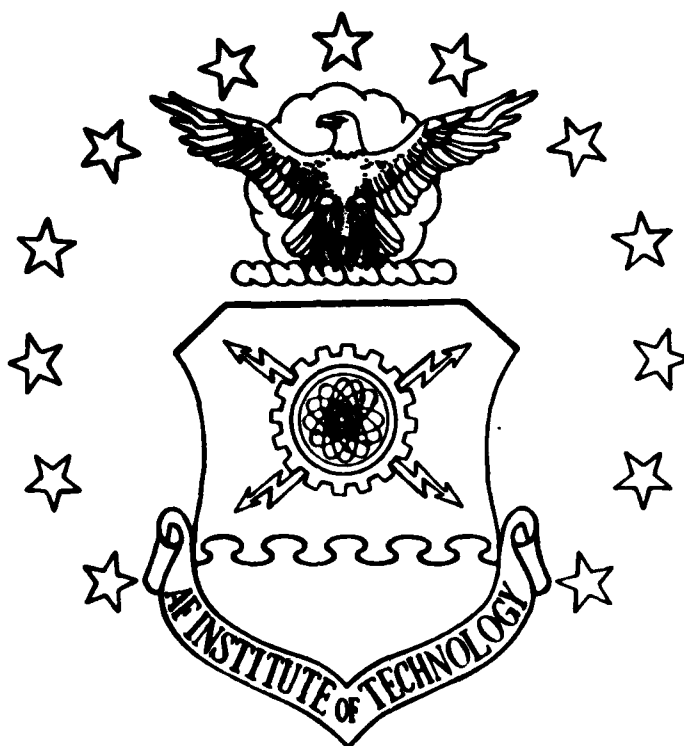
MICROCOPY CHART

AD-A167 073

SURF CE DEPLETION CORRECTION
TO CARRIER PROFILES
BY HALL MEASUREMENTS

THESIS

David W. Elsaesser
Second Lieutenant, USAF

AFIT/GEP/ENP/85D-3

DTIC
ELECTE
MAY 1 2 1986

S   D

B

DEPARTMENT OF THE AIR FORCE
AIR UNIVERSITY
AIR FORCE INSTITUTE OF TECHNOLOGY

Wright-Patterson Air Force Base, Ohio

86 5 12 035

AFIT/GEP/ENP/85D-3

SURFACE DEPLETION CORRECTION
TO CARRIER PROFILES
BY HALL MEASUREMENTS

THESIS

David W. Elsaesser
Second Lieutenant, USAF

AFIT/GEP/ENP/85D-3

DTIC
ELECTE
MAY 1 2 1986

S   D

B

Approved for public release; distribution unlimited

SURFACE DEPLETION CORRECTION TO CARRIER PROFILES

BY HALL MEASUREMENTS

THESIS

Presented to the Faculty of the School of Engineering

of the Air Force Institute of Technology

Air University

In Partial Fulfillment of the

Requirements for the Degree of

Master of Science in Engineering Physics

David W. Elsaesser, B. S.

Second Lieutenant, USAF

December 1985

PREFACE

This study has as its goal the development of procedure for correcting measured Hall carrier profiles, which have been distorted from the true carrier profiles by a surface depletion effect. All the necessary lab work was carried out at the Avionics Laboratory.

I wish to express great appreciation for the assistance and guidance of many individuals who assisted me during this study. I give special thanks to Dr. Y. K. Yeo, my thesis advisor, for his invaluable guidance. I also give heart felt thanks to C. Geesner, who deposited the encapsulants, and J. Ehret for performing the ion implantation.

<div align="right">

David W. Elsaesser

</div>

Table of Contents

List of Figures

AFIT/GEP/ENP/85D-3

ABSTRACT

A method was developed for correcting a carrier
profile by Hall Measurements for the surface depletion
effect. The method assumes that the experimental data is
to be fit with a Pearson type-IV curve.

In order to correct the measured profile it is
necessary to know the depletion width after each etch. The
depletion widths are dependent upon the real profile and
not the measured, therefore if one only has measured data,
the depletion width cannot be directly determined.   In
order to gain insight into the problem a procedure called
"reverse correction" is developed. It creates a measured
profile from a real profile.

The method for correction is the following. First
assume a real profile is known. Calculate the depletion
widths from this profile. From these depletion widths and
the Pearson type-IV fit to the original measured data
construct a new assumed real profile. Repeat this
procedure self-consistently until convergence of the
assumed real data to a stable profile. This is the true
profile. Convergence is expected in approximately 7
iterations.

SURFACE DEPLETION CORRECTION TO CARRIER PROFILES
BY HALL MEASUREMENT

I. INTRODUCTION

In recent years, the use of ion implantation as a
means of introducing impurities into a semi-insulating
semiconductor, for the purpose of device fabrication, has
been given considerable attention. For instance, active
layers in microwave FETs (Field Effect Transistors) must be
precisely controlled to depths of about 1 micron (1:14).
This requirement is difficult to meet by standard
techniques of epitaxial growth or thermal diffusion.
However, ion implantation allows one to control the doping
profile by simply varying the energy and fluence of the
incident ions. Thus, theoretically, a continuous
variation of the fluence and energy can produce any
distribution desired (2:9). In addition, ion implantation
has been found to produce good uniformity of implants over
large regions, as well as good reproducibility from wafer
to wafer (3:122).

Of particular interest is silicon-implanted GaAs,
since Si is a relatively light atom and is therefore
readily accelerated, with modest energy requirements, to
velocities necessary to produce useful implant depths.
Furthermore, it has found that low dose implants of Si in

GaAs, have produced high electrical activation efficiencies, which is more difficult to achieve with other n-type dopants such as S and Se (4:27).

There are many other applications for ion implantation which show considerable promise. For instance, in a research project conducted for NASA, Woo (5) constructed complementary-metal-oxide-semiconductor / silicon-on-sapphire circuits (CMOS/SOS) by ion implantation which were one-third faster than those fabricated by diffusion. Finally, other researchers have demonstrated the feasability of producing electrically insulating layers in device materials by ion implantation, in lieu of the more common mesa techniques (1:17).

In general, for device applications, it is necessary to accurately measure the carrier profiles of implanted semiconductors. The two common electrical means for accomplishing this are capacitance-voltage (C-V) profiling and secondly by the differential Hall method. The former makes use of a reversed biased Shottky barrier to produce a variable depletion width, determined by measuring its capacitance. As the reverse bias is increased the depletion width extends deeper into the material, decreasing the capacitance, and uncovering more dopant ions. The density of carriers at the edge of the depletion width is thus related to the differential change of capacitance with bias voltage. There are two main

disadvantages associated with C-V profiling. The first is that the profile cannot be measured inside the initial depletion width, which occurs at zero bias voltage. The second major problem is that C-V profiling is useful only in n-type materials.

Differential Hall profiling, on the other hand, may be used in both n- and p-type materials. This technique is characterized by measuring of the sheet carrier concentration in carriers/cm^2, which corresponds to the total number of electrically active carriers below the surface per unit surface area. Next, a thin layer of the implanted material is removed by a chemical etch. A subsequent measurement of the sheet carrier concentration reveals the density of activated ions in the layer which has been etched. An obvious disadvantage with this technique is that it is destructive, and therefore, measurements may not be repeated. Another serious disadvantage is that a surface depletion region, associated with the filling of acceptor-type surface electronic states (SES), results in the measurement of a profile which is not only shifted from the true profile but also contracted. This translation is due to the fact that Hall measurements make use of only mobile carriers, thus only the carriers past the edge of the depletion width are measured. Furthermore, the distortion occurs because the depletion widths are a function of carrier concentration, which, of

course, varies with depth. Small depletion widths occur where the concentration of implanted ions is large and large depletion widths where the concentration is small.

THESIS OBJECTIVE AND SCOPE

It is the objective of this research to develop a method for correcting the Hall measured profile, thereby obtaining a profile which accurately represents the distribution of free carriers. The corrected profiles will then be compared to the profiles obtained by C-V profiling.

The substrate material used was <100> oriented undoped semi-insulating GaAs. Ion implantation was carried out at room temperature at an ion energy of 100 keV. The substrates were implanted with doses of 2, 4, 6, and 8×10^{12} as well as 1 and 3×10^{13} cm^{-2}. The last dose produces degenerate conditions in the sample. The methodology developed for correcting for correcting non-degenerate doses must be easily adapted to the case of degenerate doses.

SEQUENCE OF PRESENTATION

Chapter II provides background information on ion-implantation, with an emphasis on ion range statistics. In addition this chapter explains the theoretical basis of

surface electronic states, and establishes a relationship for the depletion width. Chapter III presents the experimental procedures and reviews the methods of Hall and C-V profiling. With this preparation, chapter IV details the reasons for the distortion of the Hall profile as well as the method for correcting it. A theoretical profile is used to demonstrate the effect of surface depletion on the measured profile. Finally, Chapter V presents the experimental results, as well as conclusions concerning its success.

II. BACKGROUND

RANGE DISTRIBUTIONS

The penetration depth of an incident ion in a solid
material is governed by various factors, among which are
the mass and energy of the ion, the mass of the target
atom, the temperature of the target material, etc. The
range can be accurately determined if one possesses a
thorough knowledge of the stopping power (-dE/dx) or
specific energy loss. This differential function is
dependent on the instantaneous energy of the ion and has
two main contributions, the electronic and nuclear stopping
powers, that is,

$$dE/dx = (dE/dx)_e + (dE/dx)_n \qquad (1)$$

Electronic stopping is characterized by small angular
elastic collisions between the ion and the target atom
electrons resulting in the ionization of the material. The
nuclear stopping term is due to the collisions of the ion
with the nucleus of the target atom, where the field is
non-coulombic and "Rutherford type" scattering takes place.
Nuclear energy loss dominates at low ion energies while
electronic loss is prevelant at large ion energies
(2:9-11).

6

Lindhard, Sharff, and Shiott (LSS) have made numerical calculation of the ion range in amorphous materials by using the Thomas-Fermi interatomic potential to calculate the contribution from the nuclear energy loss term. In addition, they have computed a mean square fluctuation in the energy loss for each collision, resulting in a mean square fluctuation in the total range σ^2. This calculation of straggling.assumes, as a first approximatior a Gaussian range distribution (2:36-39). That is, the distribution of implanted ions with depth is given by

$$N(x) = \frac{\phi}{\sigma\sqrt{2\pi}} \text{EXP}\left[\frac{-(x-R_p)^2}{2\sigma^2}\right] \qquad (2)$$

Where R_p is the projected, or mean range perpendicular to the surface, ϕ is the fluence or dose in ions/cm^2, and σ is the standard deviation about the projected range. For instance, for an energy of 100 keV, the project range of Si in GaAs is 0.085 μm, with a standard deviation of 0.0442 μm. Figure 1 illustrates the LSS distribution.

However, experimental evidence has shown that depending upon the relative importance of the nuclear collision process, the distribution can be quite asymetric, necessitating higher order moments of the distribution. Another factor influencing this asymmetry is ion channelling, in which incident ion travelling parallel to or scattered in the direction parallel to a crystal

7

GAUSSIAN APPROXIMATION OF IMPURITY CONCENTRATION, $N(X_P)$:

$$N(X_P) = \frac{\phi}{\sigma_P \sqrt{2\pi}} \text{ EXP} \left(-\frac{(X_P - R_P)^2}{2\sigma_P^2} \right),$$

WHERE ϕ IS ION DOSE/CM^2, AND X_P IS A MEASURED DISTANCE ALONG THE DIRECTION OF INCIDENT ION BEAM.

$N_P = \dfrac{\phi}{\sigma_P \sqrt{2\pi}}$ at $X_P = R_P$

$N = \dfrac{1}{\sqrt{e}} N_P$ at $X_P = R_P \pm \sigma_P$

SURFACE
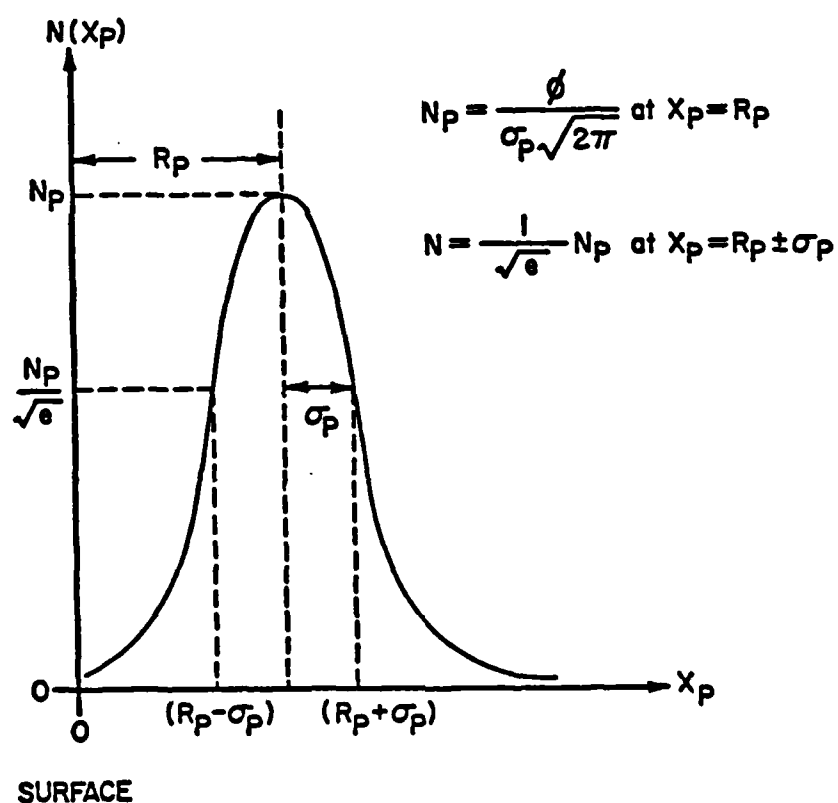
Figure 1. Typical Theoretical LSS
Ion Distribution

8

direction have a projected range much larger than expected (2:40). A distribution function which incorporates higher order moments is the Pearson type-IV, which satisfies the following relation

$$\frac{df}{dx} = \frac{(x-a)f(x)}{b_0 + b_1x + b_2x^2} \qquad (3)$$

along with the condition

$$\int_{-\infty}^{\infty} f(x)dx = 1$$

The four constants a, b_0, b_1, and b_2, are functions of the first four moments of the distribution, that is, the projected range, the standard deviation, skewness, and kurtosis. According to Hofker (6:46-47), profiles obtained from boron implanted silicon, at various energies ranging for 30 keV to 800 keV, indicate the Pearson-IV distribution to be far superior to the Gaussian distribution in fitting this experimental data.

Equation (3) may be integrated to obtain an analytic expression for the distribution. A more detailed account of the Pearson-IV distibution, including the effect of the projected range, standard deviation, skewness, and kurtosis on the shape of this distribution is given in appendix A.

9

SURFACE ELECTRONIC STATES

The theory of rectification of a metal semiconductor contact developed by Shottky implied that the maginitude and polarity of the contact potential would be quite sensitive to the work function of the particular metal used in forming the junction (7:4). However, experimental evidence shows that the contact potential is virtually unaffected by the work function of the metal. In 1947 Bardeen (7:5) proposed that the potential barrier accross the contact was produced by surface states, rather than the contact potential. The theoretical existence of surface states had been surmized earlier by Tamm and Shockley, however there impact upon the electrical properties of semiconductors was not realized until Bardeen's insight.

The existence of surface states, as explained by Shockley (8:317), is due to the sudden asymmetrical termination of the periodic potential of the crystal lattice at the surface, as shown in figure 2. Thus, the periodic boundary conditions applied in Kronig-Penny theory no longer hold at the surface. Shockley has shown that this gives rise to quantum states, localized at the surface, which have energies within the forbidden gap. Furthermore, it is also appropriate to view the surface electronic states as being due to unfilled orbitals, or dangling bonds. For instance, Massies et al. (9:640) have

Surface Electronic States   Bloch Wave Function
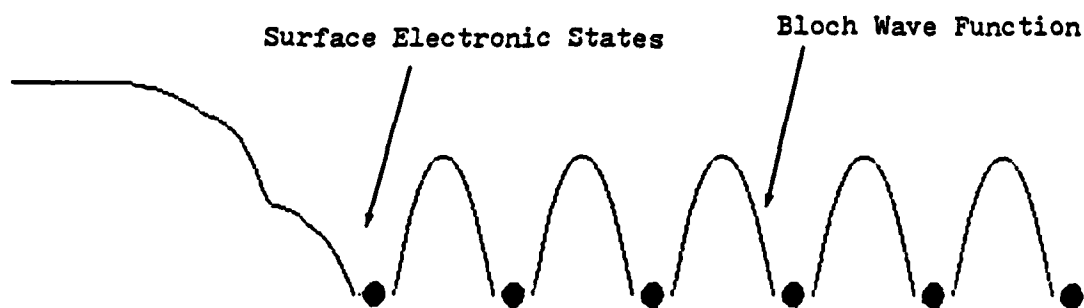
Figure 2.   Asymetric potential at
the crystal surface
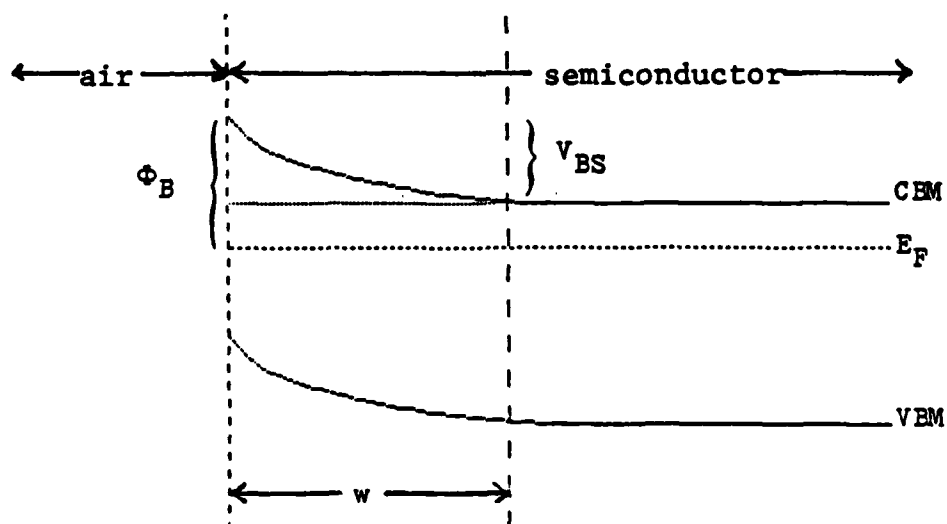
Figure 3. Band bending at the surface

observed a transition from a Ga 3d to a Ga dangling bond on
the (100) face of GaAs (9:640). Both Tamm and Shockley
have shown there to be approximately one surface state for
each surface atom.

The charging of the surface states causes the valence
band maximum and conduction band minimum to rise as they
approach the surface, as shown in figure 3. The depletion
width extends from the surface until the depth where the
bands coincide with their bulk positions. As shown by
Chandra et al. (10:646), the depletion width is given by

$$w = \sqrt{\frac{2\epsilon(V_{BS} - kT/e)}{e(N_d - N_a)}} \qquad (4)$$

where, V_{BS}, is given by

$$V_{BS} = \phi_B - \frac{kT}{e} \ln\left(\frac{N_c}{(N_d - N_a)}\right) \qquad (5)$$

In these equations, ϕ_B is the difference in the
conduction band and Fermi level at the surface in eV, and
N_c is the density of states of states at the conduction
band minimum, N_d and N_a are the concentratitions of
donor and acceptor dopants, respectively. The value of ϕ_B
for the (100) face of n-type GaAs has been measured by
Massies et al. (9:641) as well as Pianetta et al. (11:617),

12

and has been found to be approximately 0.6 eV.

In the case of degenerate statistics, equation (5) is no longer applicable, as the Fermi level moves above the conduction band minimum. Following Hattori (12:6907), the approximation that $V_{BS} = \phi_B$ when $N(x) > N_c$, will be adopted. That is, in degenerate conditions, the depletion width extends approximately to the point where th Fermi level coincides with the conduction band minimum.

III. EXPERIMENTAL PROCEDURES

SAMPLE PREPARATION

The substrate material used in this study was <100>
oriented undoped semi-insulating GaAs. The 2 inch circular
wafers were cut into 1/2 inch by 1/2 inch square samples
which were prepared for implantation. This preparation
included cleaning with basic-H, de-ionized water,
trichloroethylene, acetone, methanol, and then drying with
nitrogen gas. When dark field microscopy had revealed that
this cleaning had removed all foreign material from the
substrate surface, the substrate was free-etched with an
$H_2SO_4:30\%H_2O_2:H_2O$ solution in a 7:1:1 ratio by
volume for 3 minutes. Implantation of Si was carried out
at room temperature with an incident energy of 100 kev for
doses ranging from 2 x 10^{12} through 3 x 10^{13} cm^{-2}.
The ion beam was directed 7° off the <100> crystal axis in
order to minimize the effect of ion-channeling. After
implantation the samples were soaked in an HCl solution for
1 minute in order to remove a natural oxide layer which had
grown since implantation. The samples were then
immediately capped with a 1000 Å layer of Si_3N_4 using
a plasma enhanced deposition system. The samples were
then annealed at 850°C for 15 minutes in flowing hydrogen
gas to activate the implanted ions. This combination

14

produces high activation efficiencies, as shown by Kim (4:27), who achieved activativation efficiencies of at least 80% for 6 x 10^{12} cm^{-2} implants of silicon in GaAs. After annealing, the encapsulants were removed with a 48% Hydroflouric acid solution, which required approximately 10 minutes. Each 1/2 inch by 1/2 sample was then cut into 4 quarter inch by quarter inch samples.

Samples from each dose were then profiled using the capacitance-voltage method described below. Subsequently, several samples from each dose, with satisfactory C-V profiles, were chosen and sheet concentration measurements were made. Prior to sheet measurements indium contacts were placed on the corners of the samples, and they were then annealed at 375 °C for 3 minutes in order to produce ohmic behavior. Hall profiles were obtained from samples with representative activation efficiencies from each dose.

ELECTRICAL MEASUREMENTS

CAPACITANCE-VOLTAGE PROFILING

A rectifying metallic contact on an n-type semiconductor produces a space charge region, or depletion region, in the semiconductor. Electrons from this region are transferred to the metal, in order that the Fermi level be continuous accross the junction. If an additional

reverse bias voltage is applied to the contact, the depletion width may be extended deeper into the material. The space charge region may be treated as a voltage dependent parallel plate capacitor, with capacitance

$$C = \frac{\epsilon A}{x} \qquad (6)$$

where x is the depletion width in cm, A is the area of the contact in cm^2, ϵ is the permittivity of the material in Farads/cm, and C is the capacitance of the contact in Farads. If the reverse bias voltage is increased by dV, the space charge region extends deeper into the material by dx, which correspondingly reduces the barrier capacitance, and uncovers N(x)Adx ions at the edge of the depletion width. Henisch (13:216) has related the differential change in capacitance with bias voltage to the carrier concentration at the edge of the depletion width:

$$N(x) = 2 \left[\epsilon e \frac{d\left(\frac{A}{C}\right)^2}{dV} \right]^{-1} \qquad (7)$$

C-V profiles were obtained with the aid of the Hewlett-Packard Model 4061 A Semiconductor/Component Test System. The sample to be profiled was placed implanted face down onto two ducts. The ducts were then evacuated allowing mercury to rise to the top of each, thereby coming

16

into contact with the implanted surface. The larger duct was connected to the high side of the bias supply and the small duct was connected low side. Bias voltages from 0 V to -8 V were then incrementally applied to measure the profiles. The bias voltage was supplied with the Hewlett-Packard 4140 B DC Voltage source. The capacitance was measured at each voltage step using a 0.01 V 1 MHz test signal supplied by the 4275A Multi-Frequency LCR meter which then measured the complex impedance and thereby determined the capacitance of an assumed equivalent circuit. This circuit was comprised of the capacitance of the space charge region in series with the resistance of the material between the two mercury contacts.

HALL MEASUREMENTS

While C-V profiling makes use of static charge to determine the carrier profile, Hall measurements use only the mobile carriers. Unfortunately, the measurement of Hall voltages only reveals the total number of carriers associated with entire implanted region. Therefore, in order to obtain a depth profile of carriers, it is necessary to combine Hall measurements with etching.

Hall-effect and sheet resistivity measurements were made using the standard van der Pauw technique. This technique requires that only four contact be placed

anywhere on the periphery of a homogeneously thick simply connected sample of arbitrary shape. However, in order to correct for this arbirtary geometry L. J. van der Pauw (14:6) has shown that it is necessary to measure the voltage accross two adjacent contacts when a current is passing through the other two, as shown in figure 4a, for square geometry. In this manner, we define the resistance R_a as V_{12}/I. Similarly, R_b is defined from figure 4b. From these two, the sheet resistivity, in $\Omega/\square$, is given by,

$$\rho_s = \frac{\pi}{\ln 2} \frac{(R_a + R_b)}{2} f \qquad (8)$$

where, f is a geometrical correction factor, which is close to unity for $R_a/R_b \sim 1$. The sheet resistivity is defined more accurately by the two relations, as in Mayer (15:4077),

$$\sigma = \frac{e}{d} \sum_i n_i \mu_i d_i \qquad (9)$$

from which,

$$\rho_s = (\sigma d)^{-1} \qquad (10)$$

where d_i is the thickness of the ith layer, μ_i is the

18
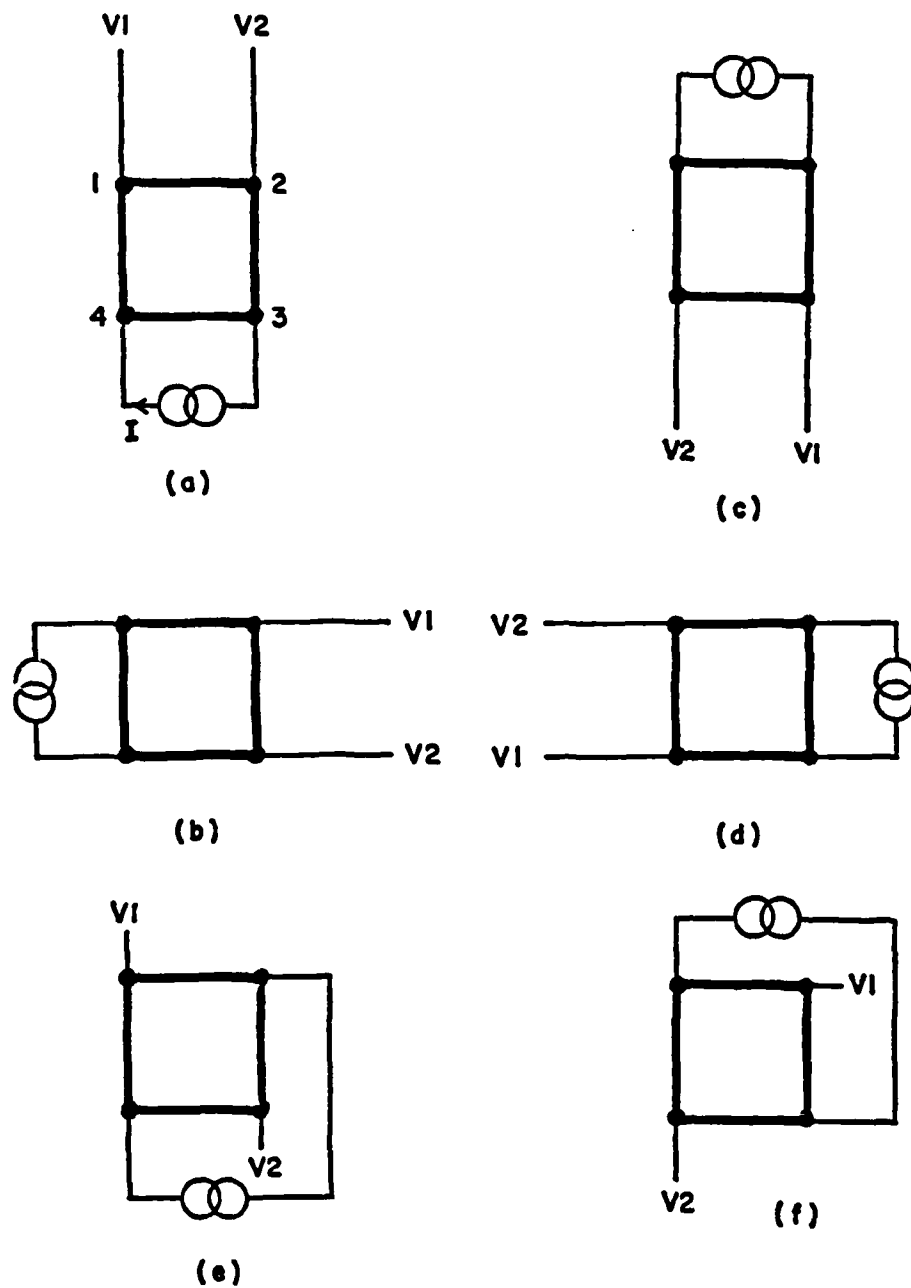
VAN DER PAUW

Figure 4. Six configurations for Hall-Effect/
sheet resistivity measurements

19

mobility in the ith layer, n_i is the carrier

concentration in the ith layer and d is the total thickness

of the implanted region. Equations (9) and (10) call

attention to the fact that as the carrier concentration

varies with depth, so does the mobility, which is only

natural, since the amount of scattering will be a function

of the impurity concentration. In equation (9), parallel

conductances at varying depths are added, to obtain the

equivalent conductance from the implanted region. Equation

(9) is then used to obtain an equivalent resistance for the

implanted region.

The sheet Hall coefficient, in $\Omega cm^2/(Vs)$, is

defined by,

$$R_s = \frac{\Delta V \; 10^8}{B \; I} \qquad (11)$$

where B is the normal component of the applied magnetic

field in Gauss, and ΔV is the change in voltage of

position (e) in figure 4, when the field is applied, and I

is the applied current in Amperes. The effective sheet

concentration, in carriers/cm^2, is given by

$$N_s = \frac{1}{e \; R_s} \qquad (12)$$

According to Petritz (16:1259), the sheet Hall

coefficient is given by,

$$R_s = \frac{\sum_i n_i \mu_i^2 d_i}{e\left(\sum_i n_i \mu_i d_i\right)^2} . \tag{13}$$

Petritz shows that this expression is correct to the first order in B. A second order term, which takes into account circulating currents, is negligible for the magnetic field used in this study, 0.5 Tesla or 5,000 Gauss.

Thus, by combining Hall-effect/sheet resistivity measurements with etching we can obtain the mobility and carrier concentration within the etched interval, that is,

$$\mu_i = \frac{\Delta(R_s/\rho_s^2)_i}{\Delta(1/\rho_s)_i} \tag{14}$$

and

$$n_i = \frac{\Delta(1/\rho_s)_i}{e\, d_i\, \mu_i} \tag{15}$$

where

$$\Delta(R_s/\rho_s^2) = \frac{(R_s)_{i-1}}{(\rho_s)_{i-1}^2} - \frac{(R_s)_i}{(\rho_s)_i^2}$$

21

and

$$\Delta(1/\rho_s)_i = (1/\rho_s)_{i-1} - (1/\rho_s)_i .$$

The quantities $(R_s)_i$ and $(\rho_s)_i$ are the sheet Hall
coefficient and sheet resistivity, respectively, which are
measured following the ith layer removal. Equations (14)
and (15) are easily obtained from the summations (10) and
(13).

Successive layers from the the implanted region are removed
using an etching solution of $H_2SO_4:H_2O_2:H_2O$ in
the ratio 1:1:100 by volume at 0 °C. Measurements were
continued until all the active layers were removed.   Black
wax, placed over the contacts prior to the first etch, and
removed after the last etch, revealed the total etched
depth. The etched depth was measured using the
Sloan-Dektak IIA Surface Profiling System, and from it an
etching rate was computed.

    A block diagram of the automated
Hall-effect/sheet-resistiviy measurement system is shown in
figure 5. It consists of a Digital Equipment PDP 11-03
computer, four Keithley Model 610 electrometers serving as
unit gain amplifiers, a Keithley Model 725 programmable
current source, a Keithley Model 6900 digital multimeter
used to measure voltages, and a Keithley Model 616 digital
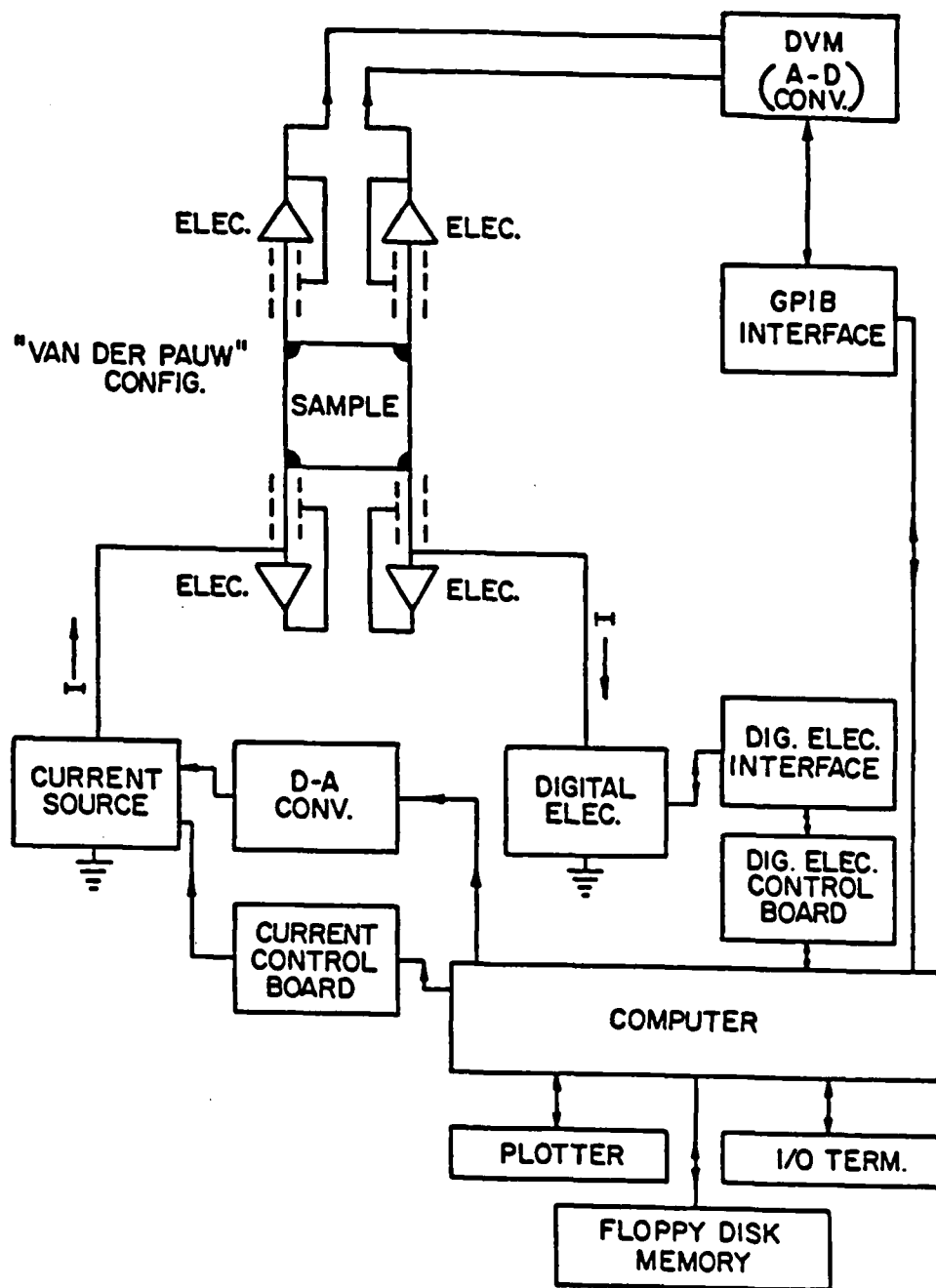
Figure 5. Block diagram of Automated Hall-Effect/
sheet resistivity measurement system.

electrometer which measures the current. As shown in figure 6, a six-position rotary switch is used to measure all the relevant parameters in each of the configurations of figure 4.
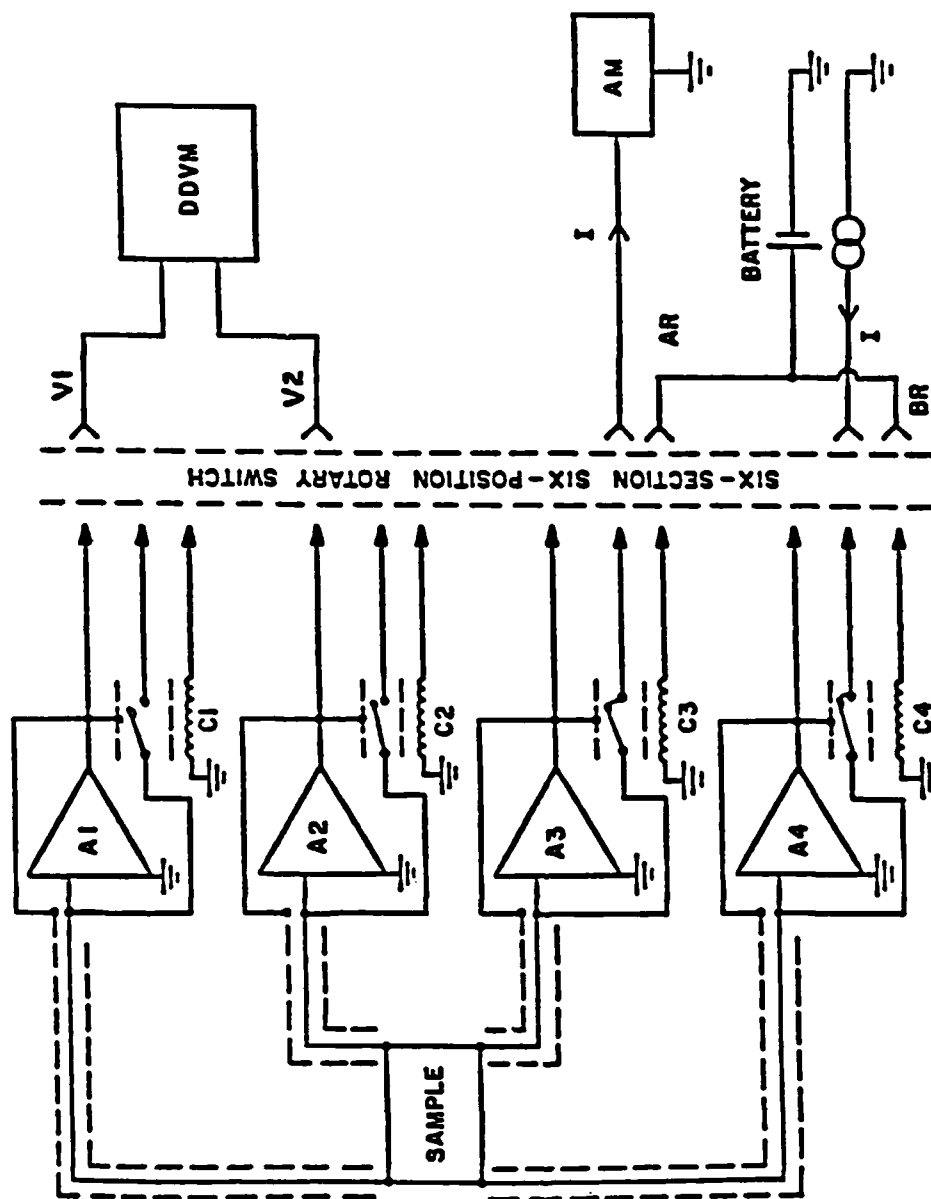
Figure 6. Schematic Diagram of the Hall measurement system using the van der Pauw Configuration

IV. THEORY

THE PROBLEM

Equations (14) and (15) which give the carrier and
mobility profiles assume that the carriers which contribute
to the summations (9) and (13) extend from the surface
through the end of the implanted region. This, however,
does not take into account the effect of surface states,
which create immobile ionized charges in the depletion
region. Therefore, these carriers do not contribute to the
Hall voltages and sheet resistances. In fact, only the
mobile carriers beneath the depletion width are detected.
That is, more properly, summations (9) and (13) should be
taken from the edge of the depletion width, $w_{\emptyset}$, through
the end of the implanted region. After an etch, there is a
new depletion width, w_1, which extends from the new
etched surface, as shown in figure 7. Although the actual
measurements were made at the depths of $w_{\emptyset}$ and w_1, this
fact was usually ignored, and the carrier concentrations
were simply calculated on the basis of etched depth,
without taking into account the surface depletion width.
When this surface depletion width is not accounted, the
measured profile obtained may be quite different than the
true profile.

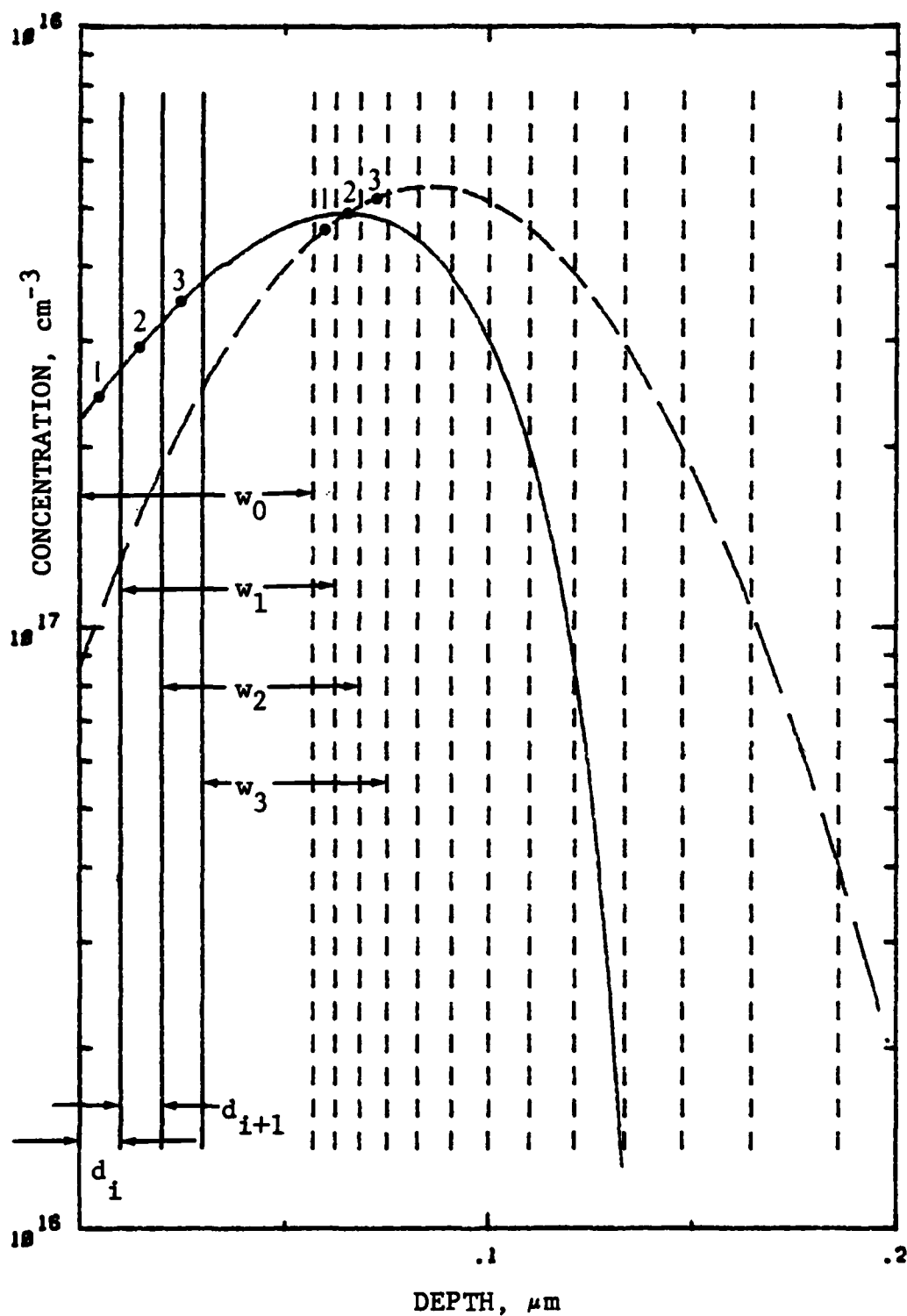Thus, we distinguish between the real and the apparent

26

Figure 7. Depletion widths vs. depth - LSS 6×10^{12}

profiles, the latter being obtained from equation (15).
From equation (14) it is obvious that the apparent mobility
profile does not depend upon the etched depth, and hence it
is simply the real mobility profile translated towards the
surface by the depletion width:

$$\mu_r(x + w) = \mu_m(x) \tag{16}$$

However, the relationship between the real and
apparent carrier profiles is not as simple. In fact, the
d_i in the denominator of equation (15) should be replaced
by $d_i + (w_i - w_{i-1})$. Here, d_i is the depth of the
ith etch, w_i is the depletion width after the ith etch,
and w_{i-1} is the depletion width after etch (i-1). This
correction acknowledges the fact that the depletion width
changes with each etch due to the non-uniform implant.
Thus, the measured concentration in equation (15) is
related to the real concentration by

$$n_r(x+w) = \frac{n_m(x)d_i}{d_i + (w_i - w_{i-1})}$$

or

$$n_r(x+w) = \frac{n_m(x)}{1 + \frac{(w_i - w_{i-1})}{d_i}} \tag{17}$$

where w is taken to be the average of the ith and the

(i-1)st depletion width. A differential relation may be obtained by allowing d_i to approach zero, that is:

$$n_r(x + w) = \frac{n_m(x)}{1 + \dfrac{\partial w(x)}{\partial x}} \qquad (18)$$

Equation (18) indicates that the true profile may be obtained from the measured profile if the function $w(x)$ is known. This function, however, is determined by the real profile, where only the measured profile is known. To gain insight into the problem, it is instructive to calculate an apparent profile from a true one, or in other words to "reverse correct".

REVERSE CORRECTION

If the real profile is known, the measured profile may be calculated with the aid of (18), (4), and (5). Equations (4) and (5), which apply to a constant concentration, are adapted to depth dependent concentrations by taking the average concentration within the depletion width. Thus, the depletion width can be self-consistently determined in conjunction with equations (4) and (5). Specifically, the average carrier concentration within the ith depletion width is given by

29

$$N_{avg} = \int_{x_i}^{x_i + w_i} N(x)\,dx/w(x) \tag{19}$$

where x_i is the distance etched from the surface, and w_i is an assumed depletion width from the ith etched surface. The average value is then inserted into equations (4) and (5) to obtain a new estimation of the depletion width w_i. Equation (19) is re-evaluated for the new w_i, yielding an updated average concentration and depletion width. This procedure is repeated until convergence to the actual ith depletion width. This usually requires approximately 5 iterations for an accuracy of one thousandths of the depletion width. With all the w_i's calculated the measured profile may be obtained from

$$n_m(\overline{x}_i) = \frac{\displaystyle\int_{x_{i-1}+w_{i-1}}^{x_i + w_i} N(x)\,dx}{x_i - x_{i-1}} \tag{20}$$

where

$$\overline{x}_i = (x_i + x_{i-1})/2$$

The reverse correction was carried out for the theoretical LSS distributions corresponding to the doses 2, 4, 6 and 8 $\times 10^{12}/cm^2$ and 1 $\times 10^{13}/cm^2$. The results are shown in figures 8 through 12. From these we
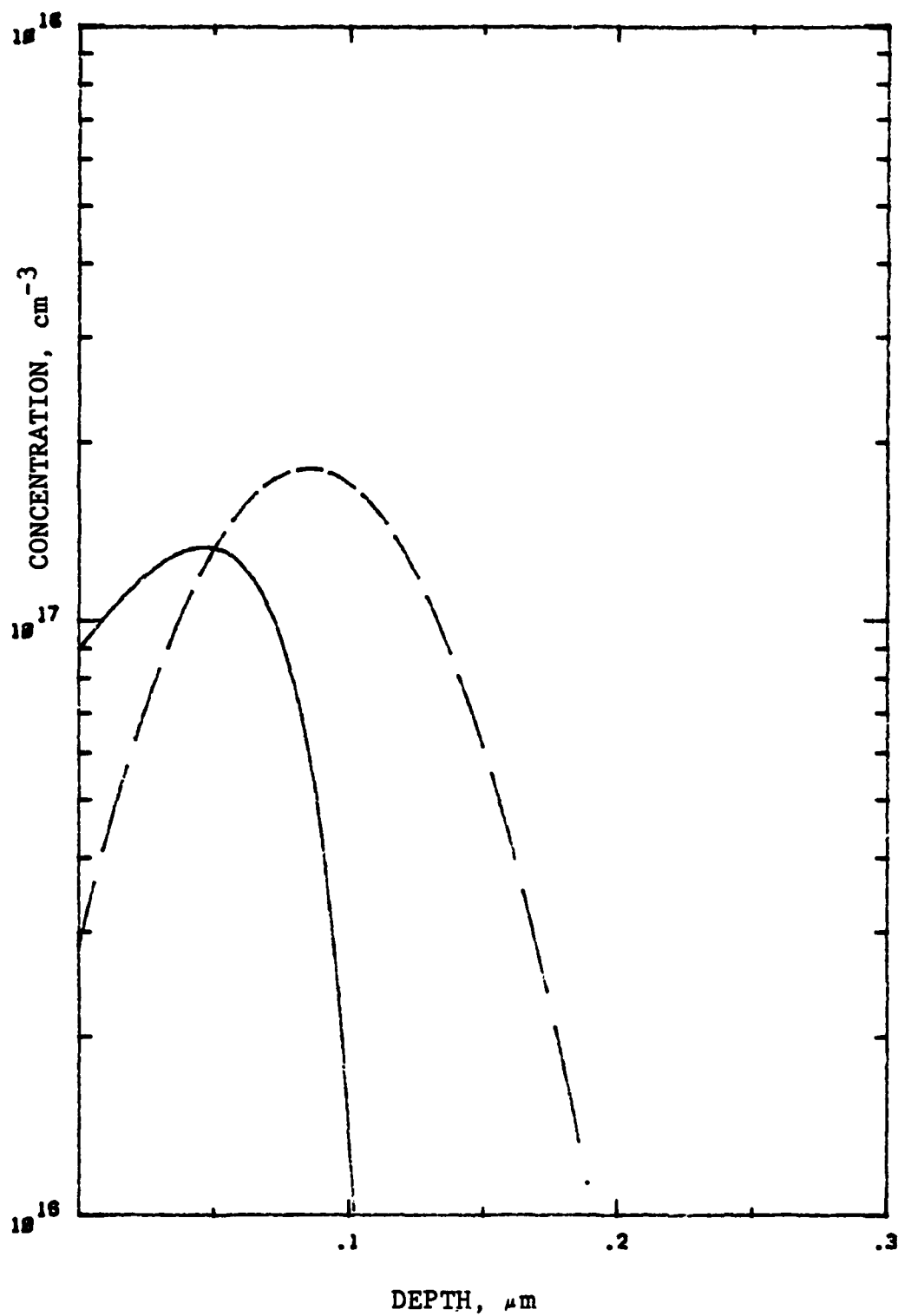
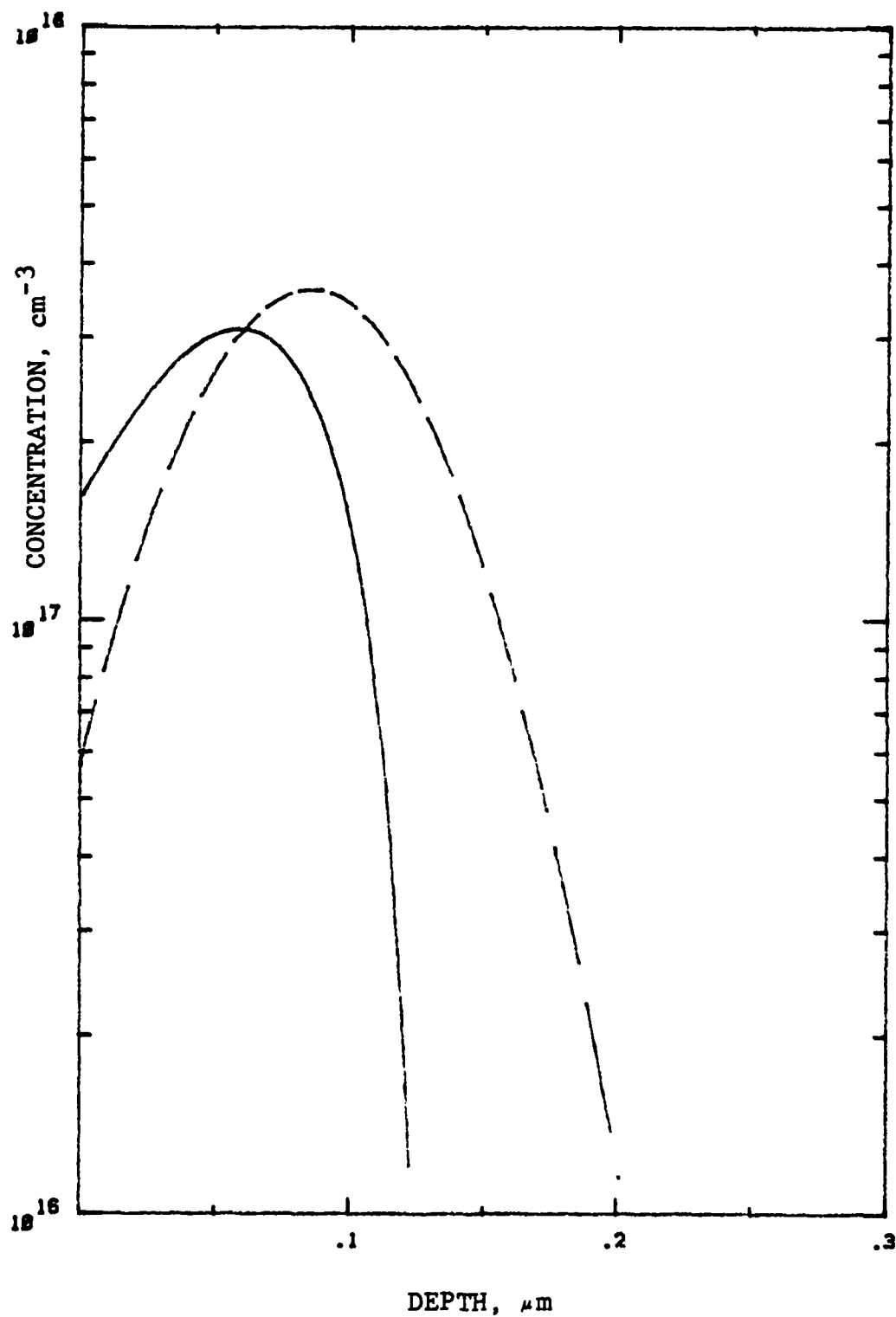Figure 8. Real and Apparent Profiles - LSS 2×10^{12}

31

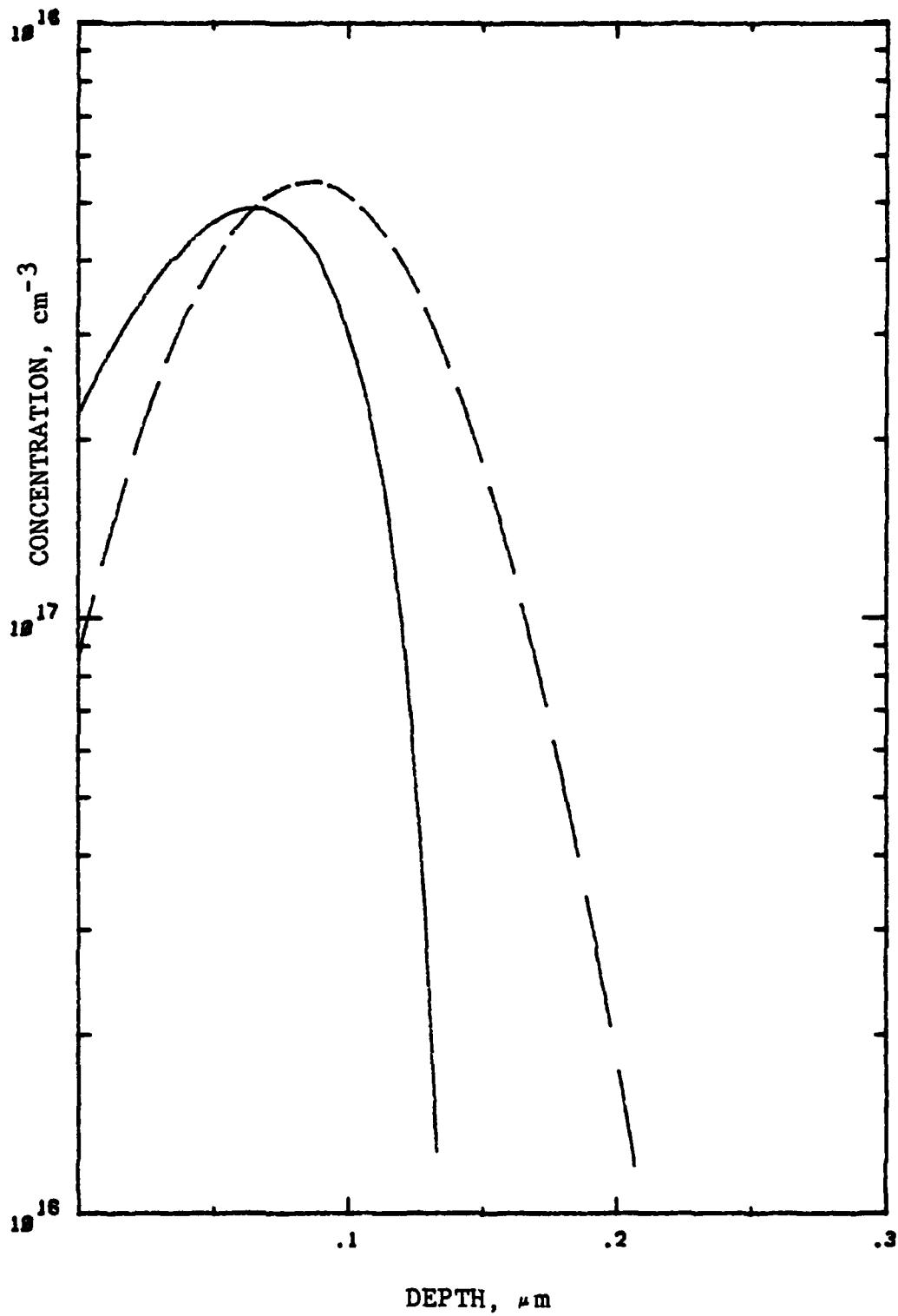Figure 9. Real and Apparent Profiles - LSS 4×10^{12}

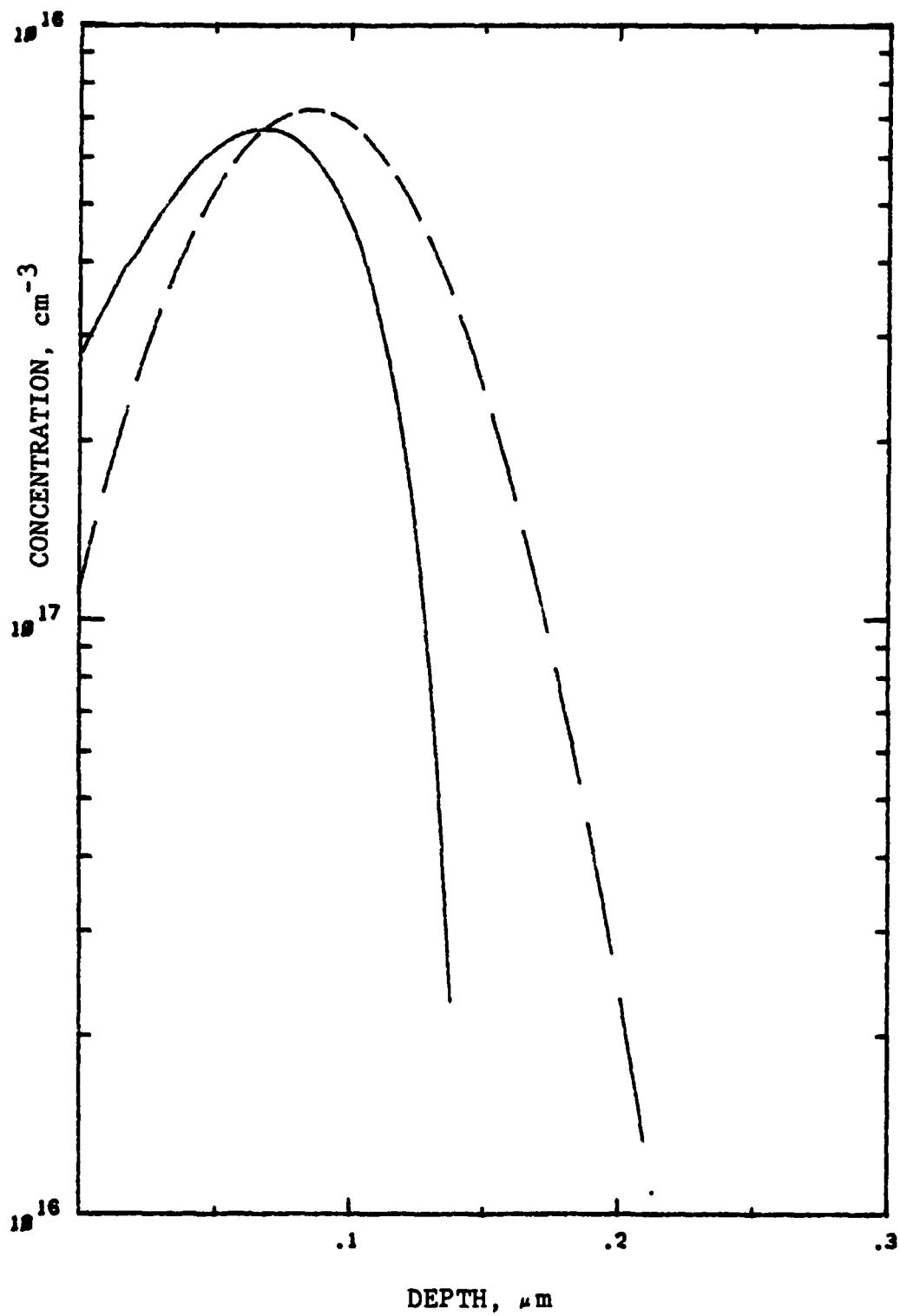Figure 10. Real and Apparent Profiles - LSS 6×10^{12}

33

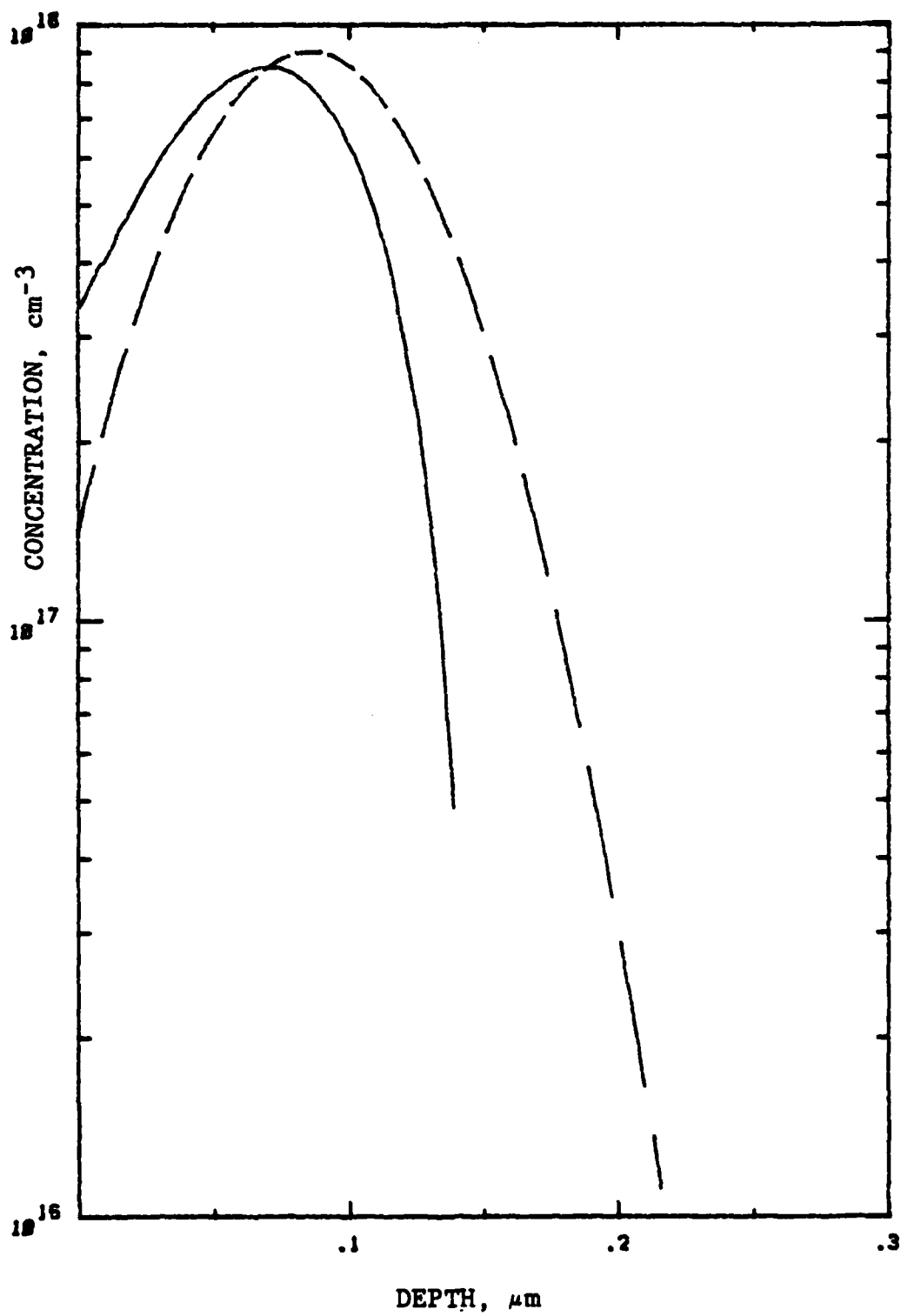Figure 11.   Real and Apparent Profiles - LSS 8×10^{12}

34

Figure 12.   Real and Apparent profiles - LSS 1x10^{13}

35

make several observations concerning the effect of surface depletion on the measured profile. First, the peak of the distribution is shifted in towards the surface, since the edge of the depletion width passes it much earlier than expected. Secondly, all the measured distributions are contracted with respect to the real profiles, for basically the same reason. Third, the distortion for lower doses is much more significant than that for higher doses. And finally, the trailing edge of each measured profile drops very sharply. The reason for this effect may be seen in figure 7 which shows the etched surfaces and their corresponding depletion width, for a dose of $6 \times 10^{12}/cm^2$. As seen in the last few etches, the depletion width is increasing rapidly, however the concentration within adjacent depletion widths is decreasing much more rapidly. This leads to the sharp trailing edges shown in figures 8 through 12. Such behavior is observed in profiles measured with the Hall method, while C-V profiles show a longer tail in the distribution.

DEPLETION WIDTH CORRECTION

Reverse correction is a straight forward procedure, since we have the true profile, from which the depletion widths are generated. Yet, in actual experimental work, we

36

only have the measured profile. The procedure, to be developed below, for calculating the true profile from the measured one, shall be known as "surface depletion width correction".

Equation (18) indicates that if the depletion width after each etch is known then the problem is solved. A first order guess for these depletion widths may be obtained by assuming a real profile, and calculating from it the depletion widths for the measured profile. Using equation (18), a first approximation to the real profile may be obtained. This profile is certainly closer to the true profile than is the measured, since no depletion widths were used in the calculation of the measured profile. This first approximation is, of course, not the true profile. It may be checked for closeness by "reverse correction". If the "reverse corrected" and measured profiles coincide then the assumed real profile is, in fact, the real profile. If the measured and "reverse corrected" profiles do not sufficently agree, then a new set of depletion widths are obtained from the latest assumed real profile and an updated real profile is again created. Convergence of this procedure is expected on the basis that the assumption of an incorrect real profile will cause a perturbing effect on the next calculated profile towards the true profile. The assumed real profiles will continually change until the only possible stable situation

37

is obtained, in which one profile agrees with next
calculated profile. This means that the calculated
depletion widths are self-consistent and thus do not change
if the reverse correction procedure is repeated. A reverse
correction of the final profile should prove this to be the
case.

The correction of actual measured profiles was
obtained with the aid of a computer program in BASIC
listed in appendix B. The procedure for correction is the
following. The measured data is fit with a Pearson-IV
curve, the parameters of which constitute the measured
profile. As a first guess to the real profile, the
measured profile is shifted in depth by the depletion width
corresponding to the maximum in its concentration. From
this assumed real profile an updated profile is then
created. This data is then graphically fit with aid of a
Houston plotter to another Pearson-IV distribution. From
this curve, another corrected distribution is obtained.
The procedure is repeated until the assumed profile is
stable, and the reverse corrected profile agrees
sufficiently with the original measured data. "Agrees
sufficiently" might be taken to mean that the reverse
correction lies within the experimental error of the
original measured data.

V. RESULTS AND DISCUSSION

The results of the corrections for each dose is shown on graphically in subsequent pages. There are three plots for each profile. The first page (Fig (a)) shows the measured data, plotted as circles, along with its Pearson-IV fit . Figure (a) also shows the final corrected Pearson-IV distribution, which represents the real profile. The depletion widths calculated from this profile are used to correct the measured data, which are then plotted as triangles, scattering around the corrected Pearson-IV profile. The depletion widths are also used to correct the mobilities, shown in the bottom of the graph as squares.

The second page (Fig (b)) shows the original measured data and the reverse corrected profile from the assumed real profile. In each of the doses, the reverse corrected profile sufficiently fits the measured data, so that we may conclude that the iteration procedure has indeed produced the real profile, and thus, the correction method is a success. Convergence of the assumed real profile to the final true profile usually required approximately 7 iterations of the correcting procedure. However it was found that lower doses were more difficult to correct. The reason for this is that the initial depletion width takes up more of a substantial part of the profile. Thus, when the newly created data, which extends from some initial

depletion width, is fit to a Pearson-IV curve, there is more uncertainty of how well the Pearson-IV fits the true profile within the depletion width. There is, however, no uncertainty about whether or not an assumed Pearson distribution is the actual real profile, since a reverse calculation will immediately reveal that it either does or does not match the original measured data.

On the final page (Fig (c)) is plotted the corrected data, along with the assumed the Pearson-IV fit, the C-V data and finally the LSS distribution for the particular dose. All three should be fairly close as each represents the real profile. This is, however, not the case. In each case the C-V profile is below the corrected Hall profile, and both the C-V and Hall profiles are much broader than the LSS with much lower peaks.

By integrating the corrected profile to the depletion width we can find the approximate density of surface states. If this value is added to the original sheet concentration, a better approximation of the electrical activation efficiency may be obtained. Table I summarizes the number of surface states, the previous activation efficiency, and the corrected activation efficiency for all the samples below. From the apparent and real activation efficiencies it is obvious that the higher the dose the less drastic are the changes in the measured and real profiles, as expected. However, note that for

TABLE I.

ACTIVATION EFFICIENCY AND SURFACE STATE DENSITY

The apparent activation efficiency, from the initial measured sheet carrier concentration, as well as the corrected activation efficiency, due to the addition of the surface state density, are presented here for each dose that was measured.

DOSE cm^{-2}	SURF. STATES, cm^{-2}	APP. ACTIV. EFF. (%)	REAL ACTIV. EFF. (%)
2×10^{12}	1.06×10^{12}	25.51	78.54
4×10^{12}	9.41×10^{11}	39.62	64.23
6×10^{12}	7.78×10^{11}	27.89	40.86
8×10^{12}	9.06×10^{11}	25.56	36.89
1×10^{13}	8.73×10^{11}	21.74	30.48
3×10^{13}	1.38×10^{12}	35.79	40.40

2×10^{12} cm^{-2} the activation efficiency increases three
fold. It is also noted from Table I that the density of
surface states appears to be independent of dose, with
statistical fluctuations around approximately
9×10^{11} cm^{-2}.

Since there seemed to be a good deal of discrepancy
between the C-V and Hall profiles, the Hall data and C-V
data from a sample with high electrical activation are
compared with a non-electrical means of profiling, namely,
Secondary Ion Mass Spectrometry (SIMS). The Hall and SIMS
data for a sample of fluence 6×10^{12} cm^{-2} were taken
from Yeo et al. (17), and a C-V profile was made to compare
with this data. The data is presented in the same form as
above, in figures 19 (a) through (c), except that
mobilities are excluded and the SIMS profile is included.
The results shown in figure 19 (c) are very interesting.
The C-V profile has almost the same shape as the corrected
Hall profile, and yet is much smaller in magnitude. On the
other hand, the SIMS data has almost the same peak
concentration as the corrected Hall profile, however it is
shifted towards the surface. Erroneous measurements of the
sputtering rate for the SIMS data and the etching rate for
the Hall data could possibly account for this slight shift
and drop in peak concentration.

O   O   O   O   O   Measured Hall Data

△   △   △   △   △   Corrected Hall Data

◻   ◻   ◻   ◻   ◻   Corrected Mobilities

x————x——x——x———x   C-V Profile

▣—▣—▣—▣—▣   SIMS Profile
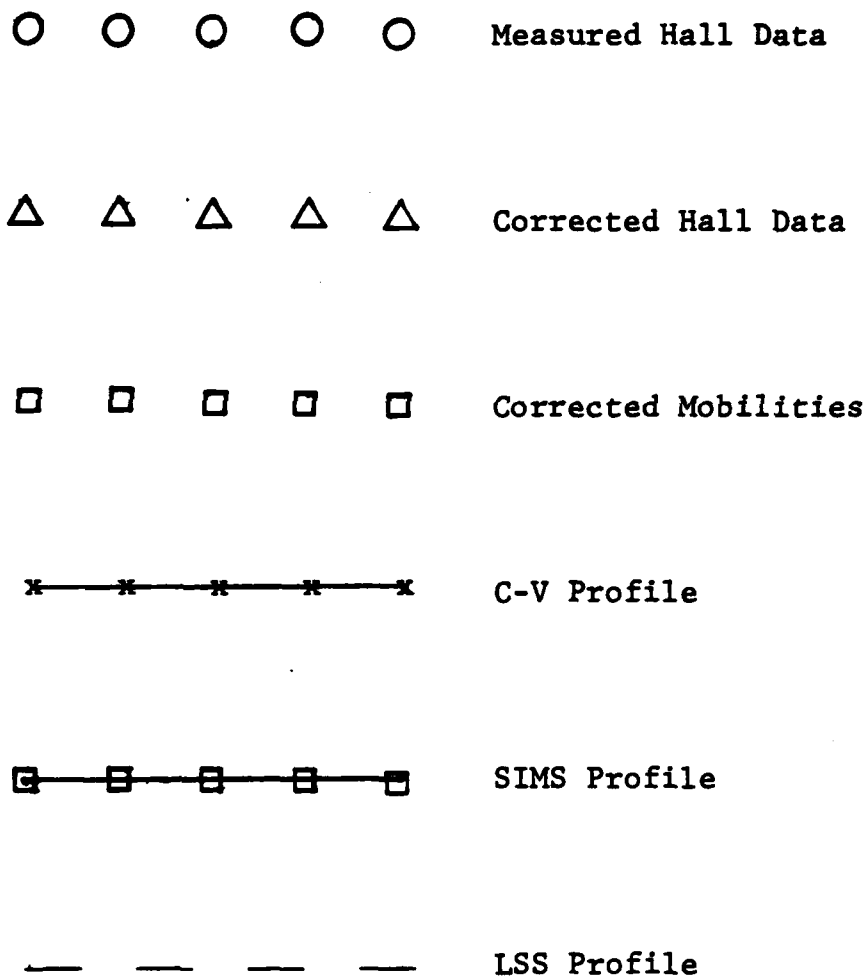
— — — —   LSS Profile

Figure 13. Symbology for Measured and
Corrected Data

43

Figure 14 a. 4×10^{12}: Apparent and Corrected Profiles

44

Figure 14 b. 4×10^{12}: Reverse Correction

45
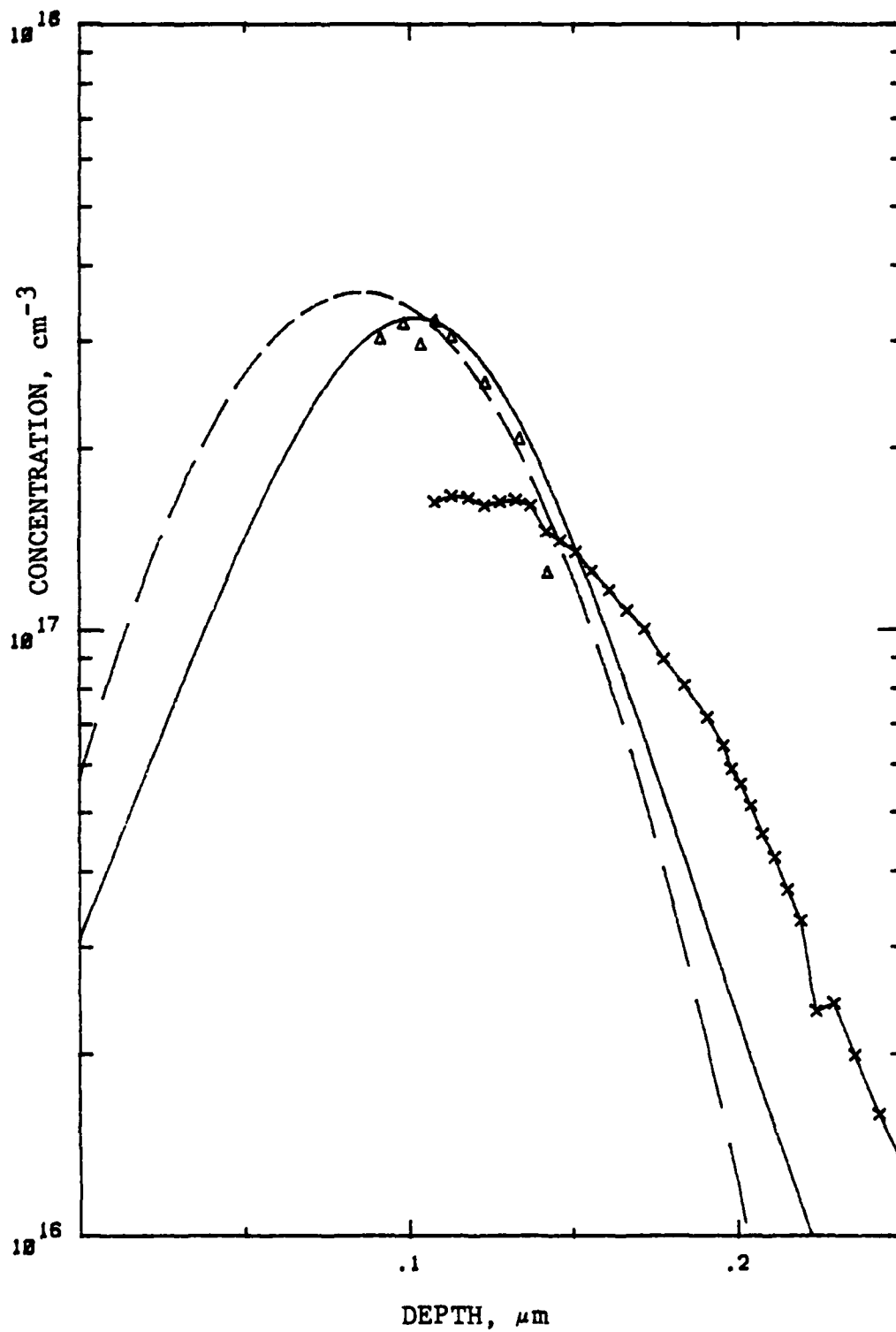
Figure 14 c. 4×10^{12}:LSS, C-V, and Hall profiles
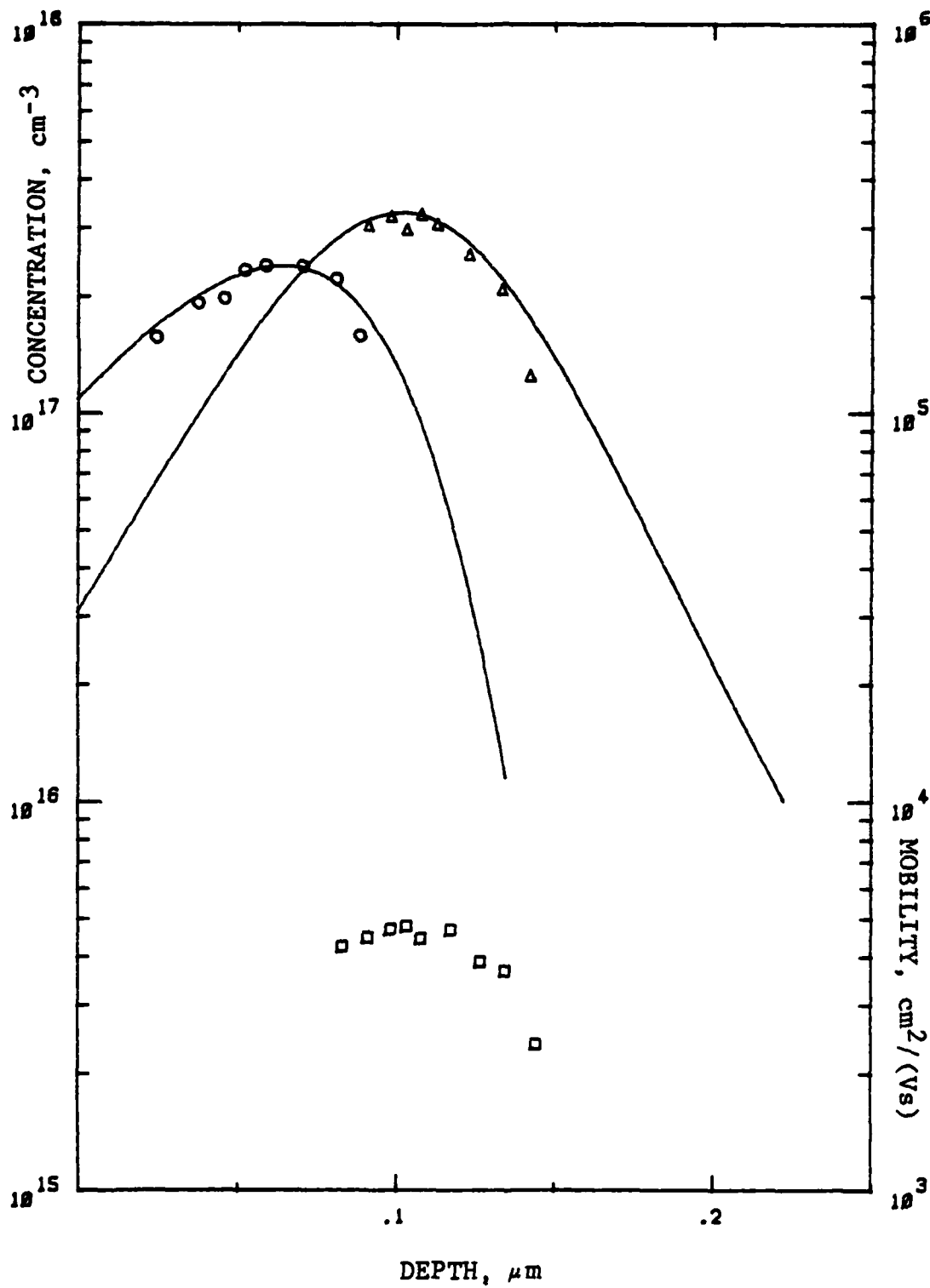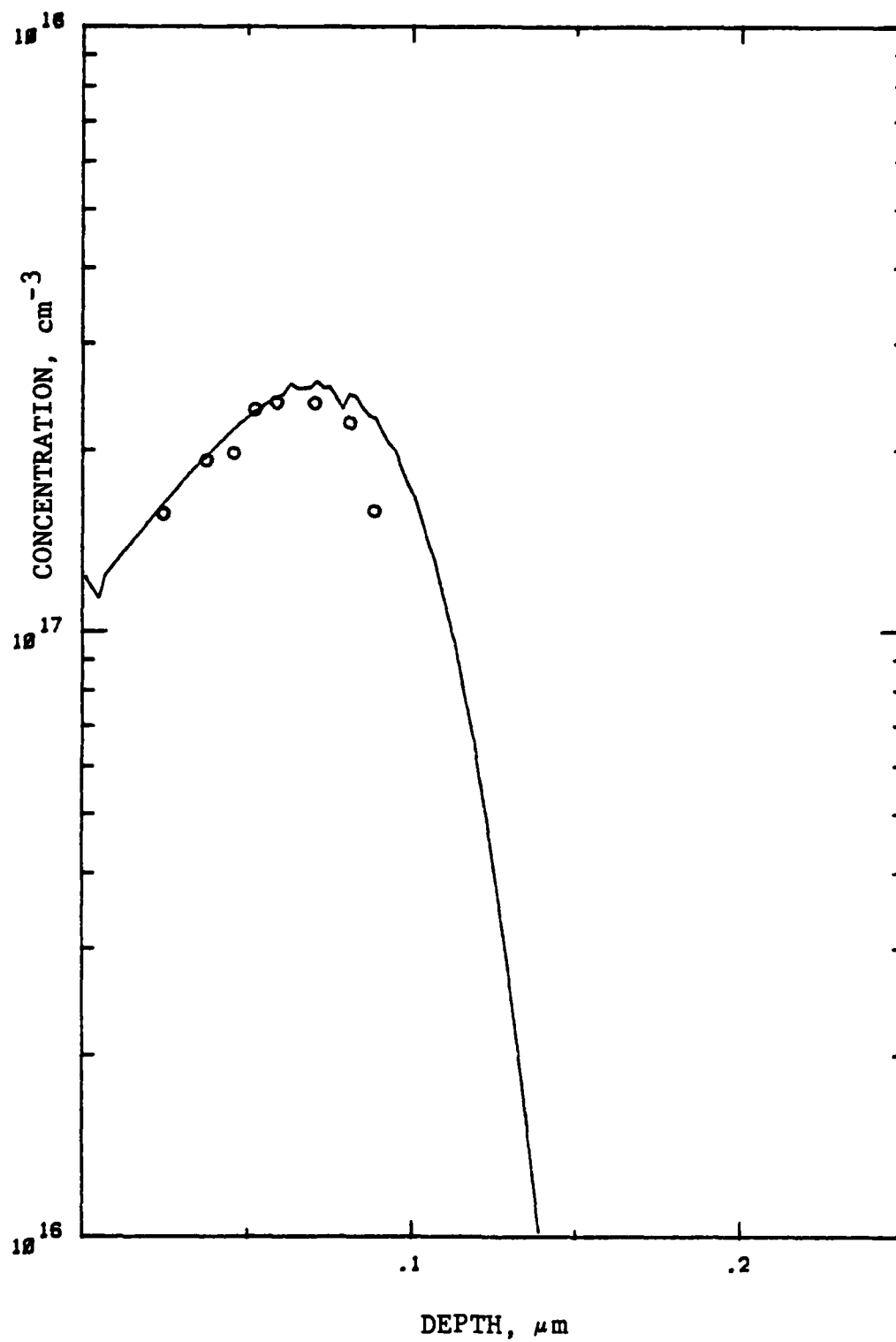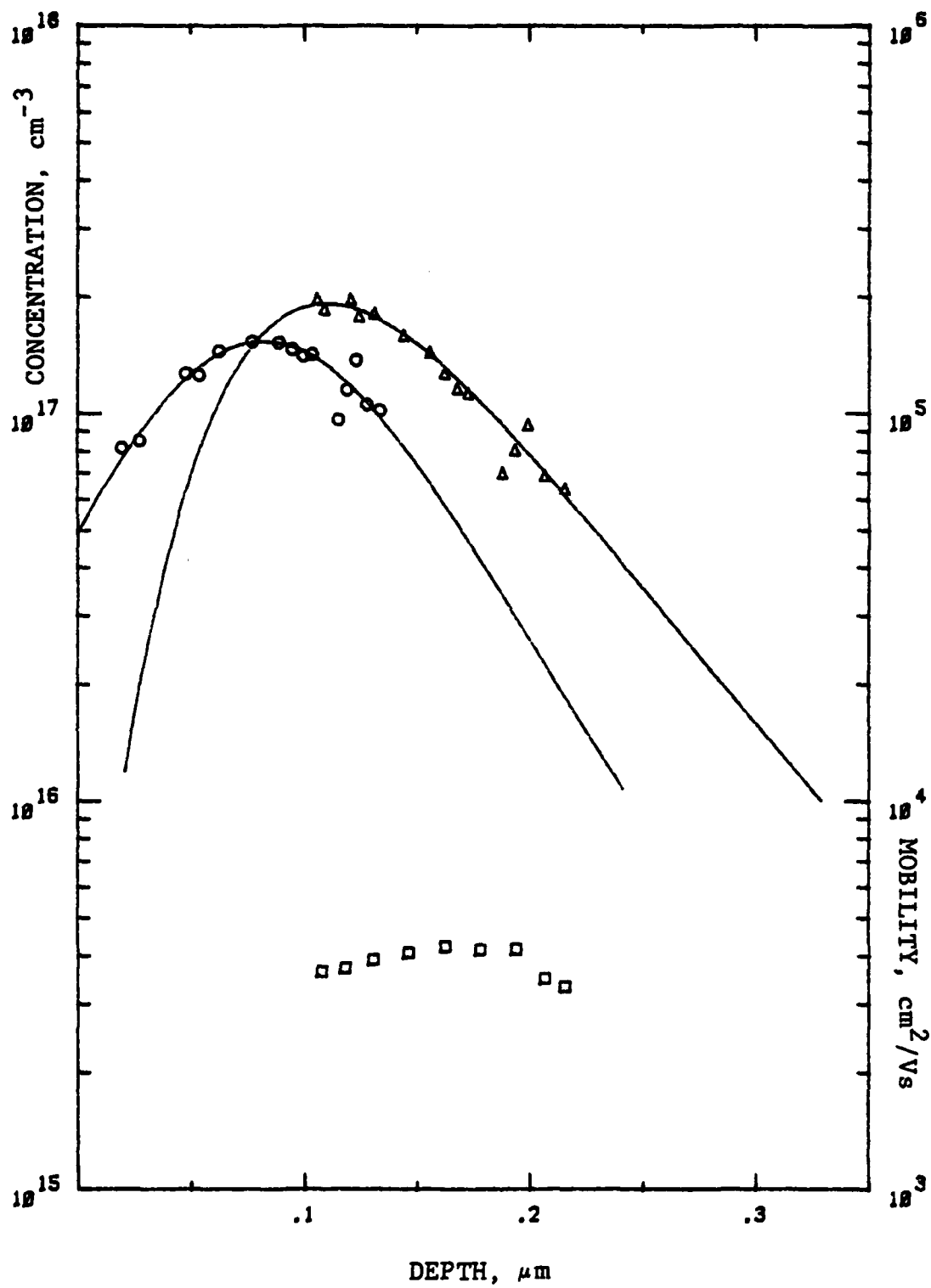
Figure 15 a. 6×10^{12}: Apparent and Corrected Profiles

47
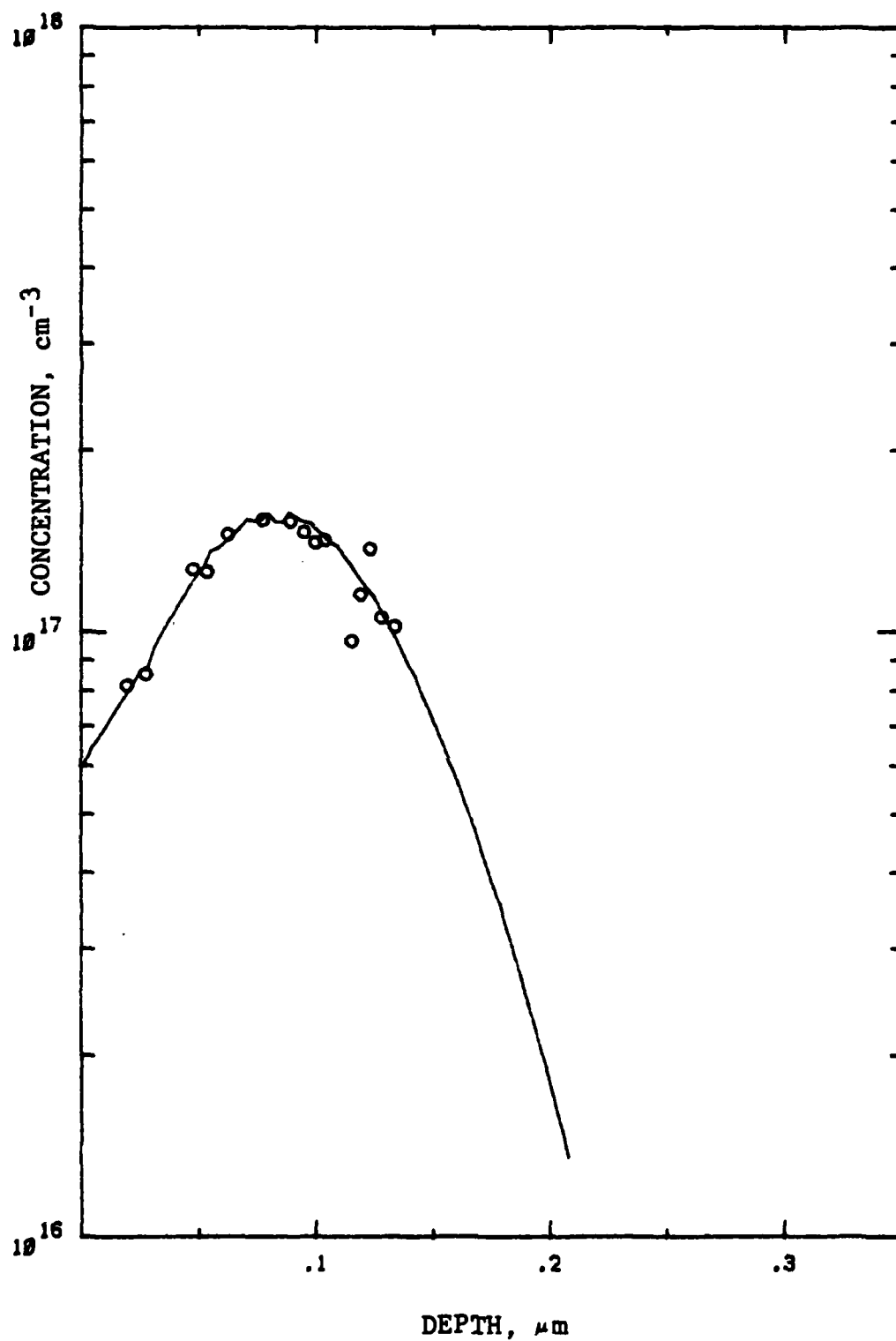
Figure 15 b. 6×10^{12}: Reverse Correction

Figure 15 c. 6×10^{12}: LSS, C-V, and Hall profiles

49

Figure 16 a. 8x10^{12}: Apparent and Corrected profiles

Figure 16 b. 8x10^{12}: Reverse Correction

Figure 16 c. 8x10^{12}: LSS, C-V, and Hall Profiles

CONCENTRATION, cm^{-3}

DEPTH, μm

10^{18}

10^{17}

10^{16}

.1 .2 .3 .4

Figure 17 a. 1x10^{13}: Apparent and Corrected Profiles
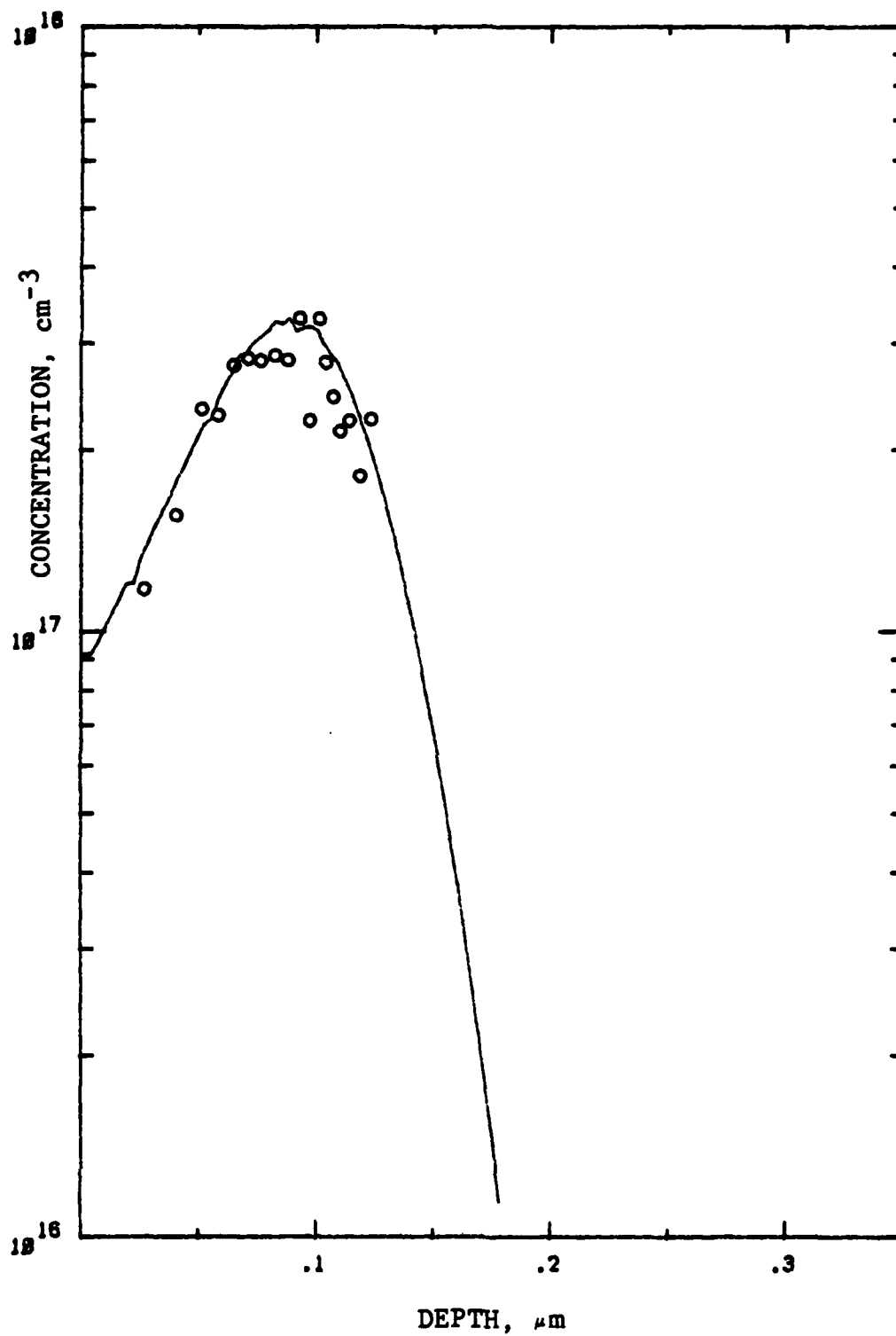
Figure 17 b. 1×10^{13}: Reverse Correction
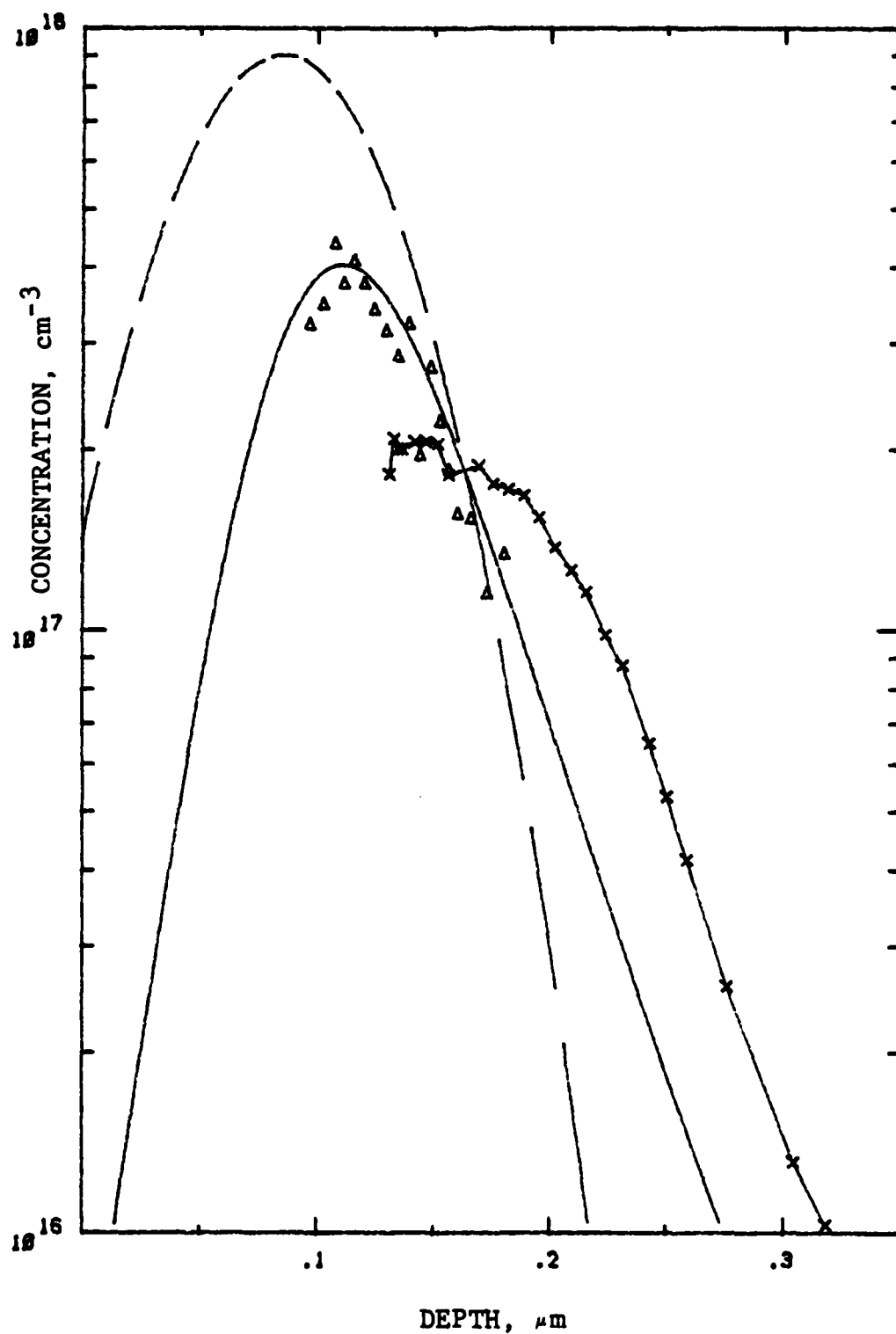
Figure 17 c. 1x10^{13}: LSS, C-V, and Hall Profiles

55
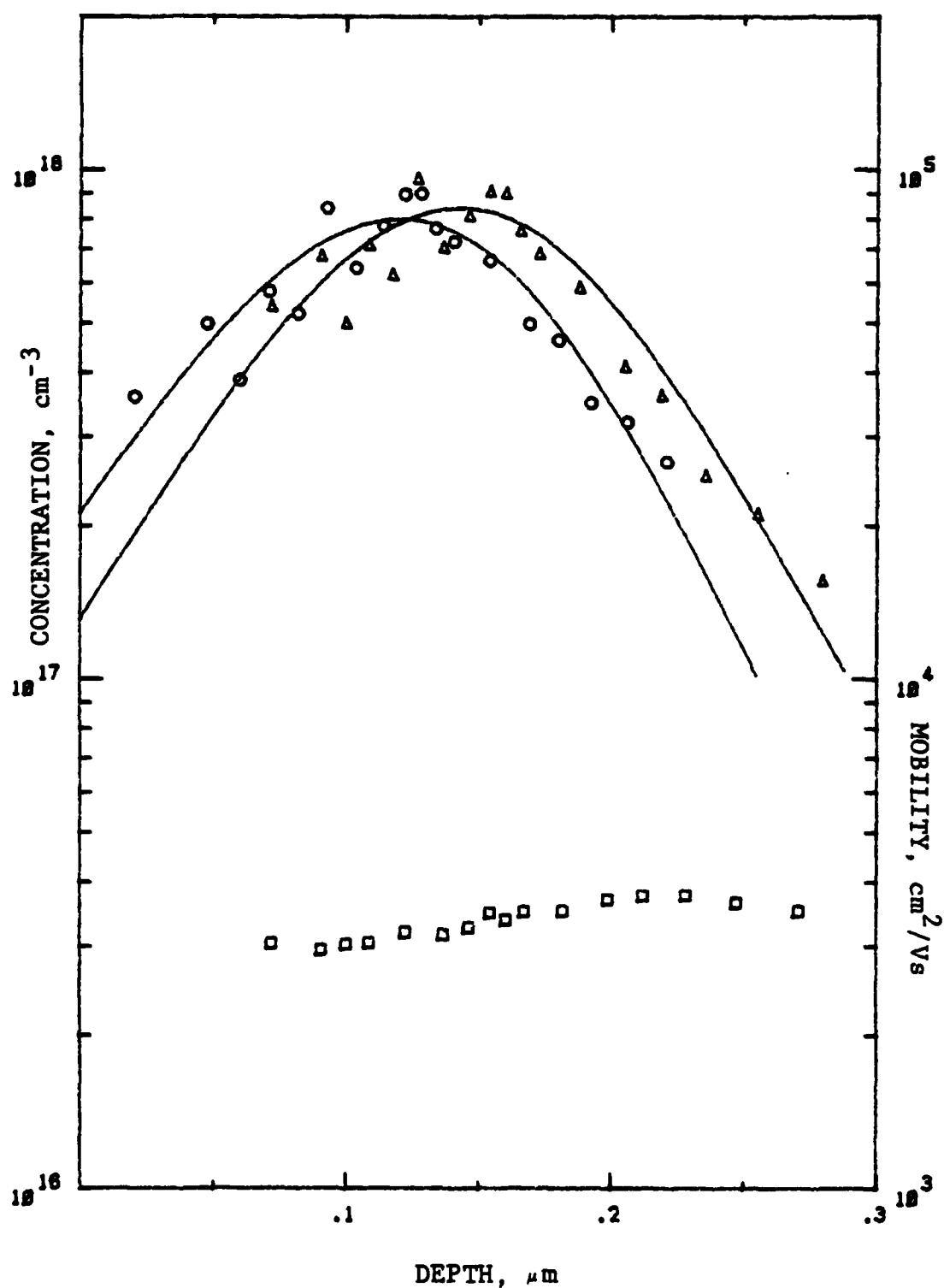
Figure 18 a. $3x10^{13}$: Apparent and Corrected profiles

Figure 18 b. 3×10^{13}: Reverse Correction

CONCENTRATION, cm^{-3}

DEPTH, μm
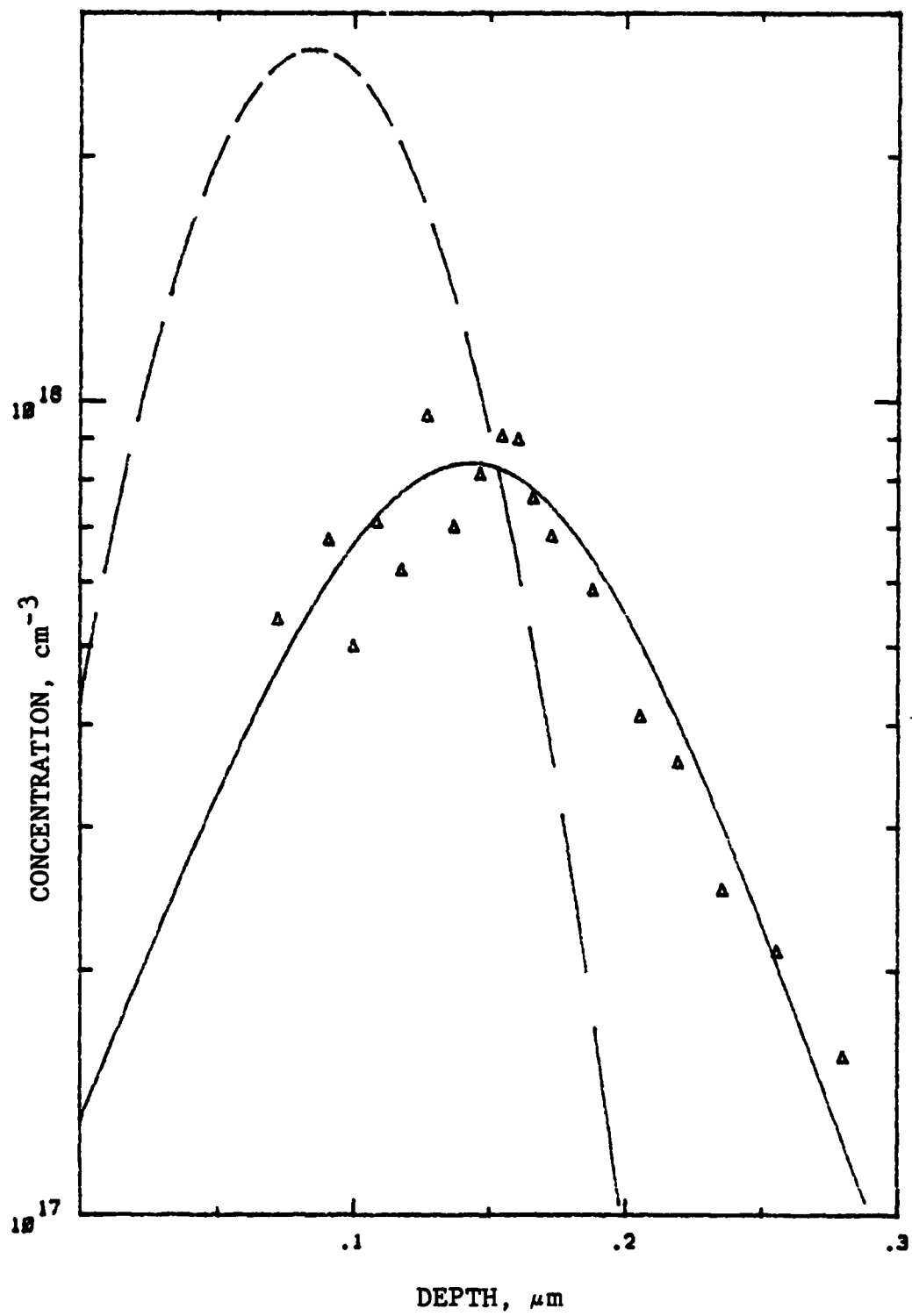
Figure 18 c. 3×10^{13}: LSS and Hall Profiles

58
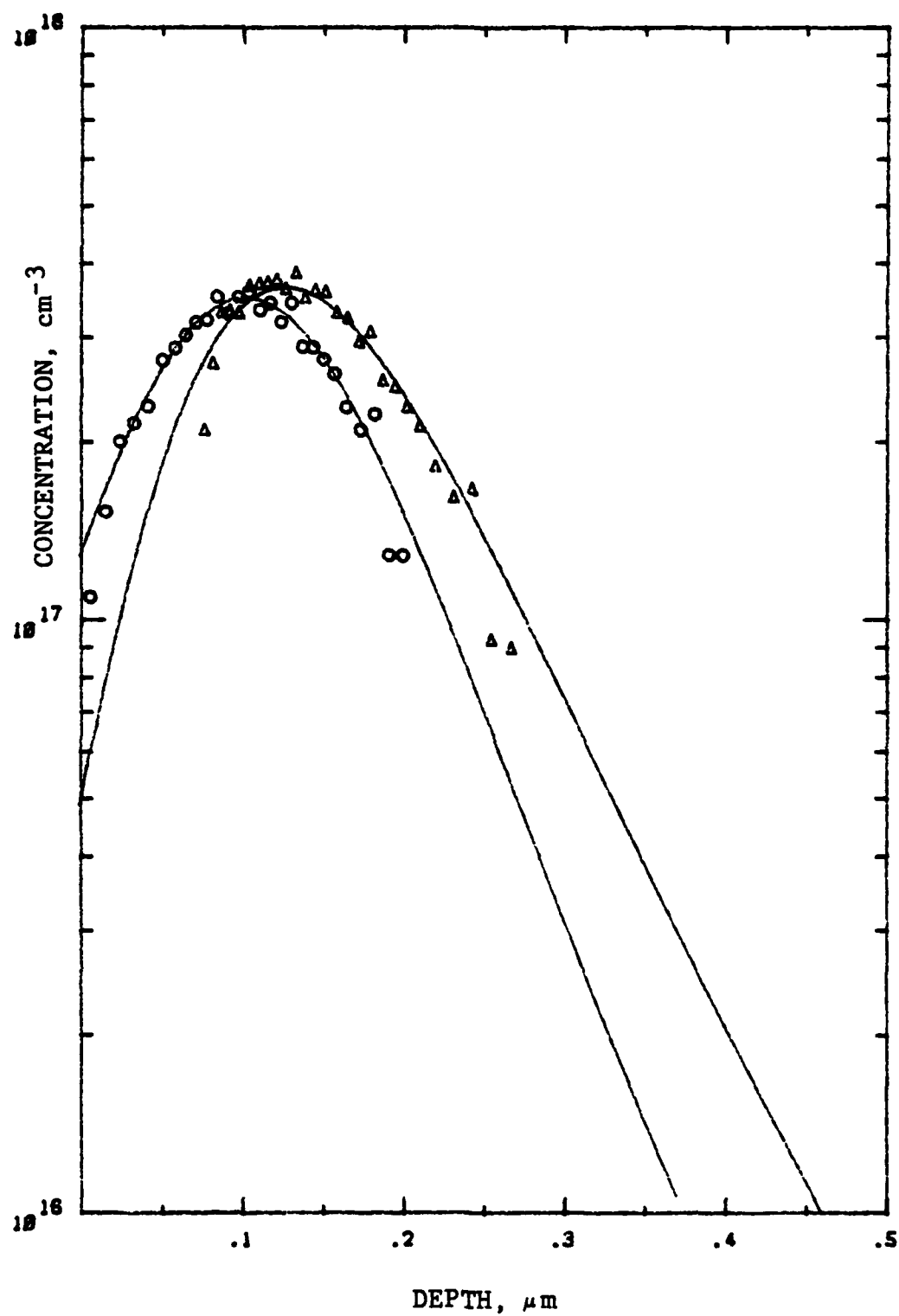
Figure 19 a. 6×10^{12}: Apparent and Corrected profiles

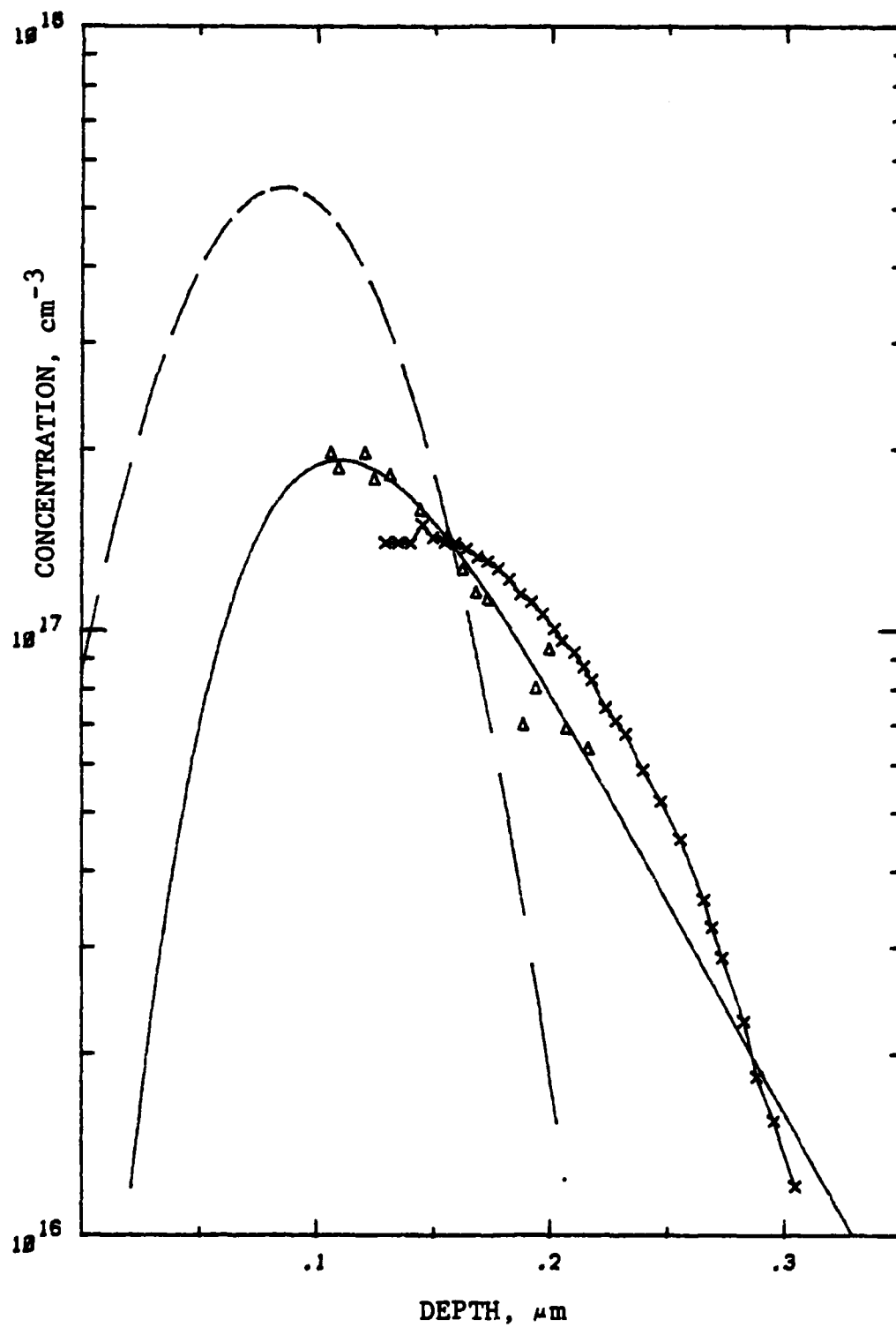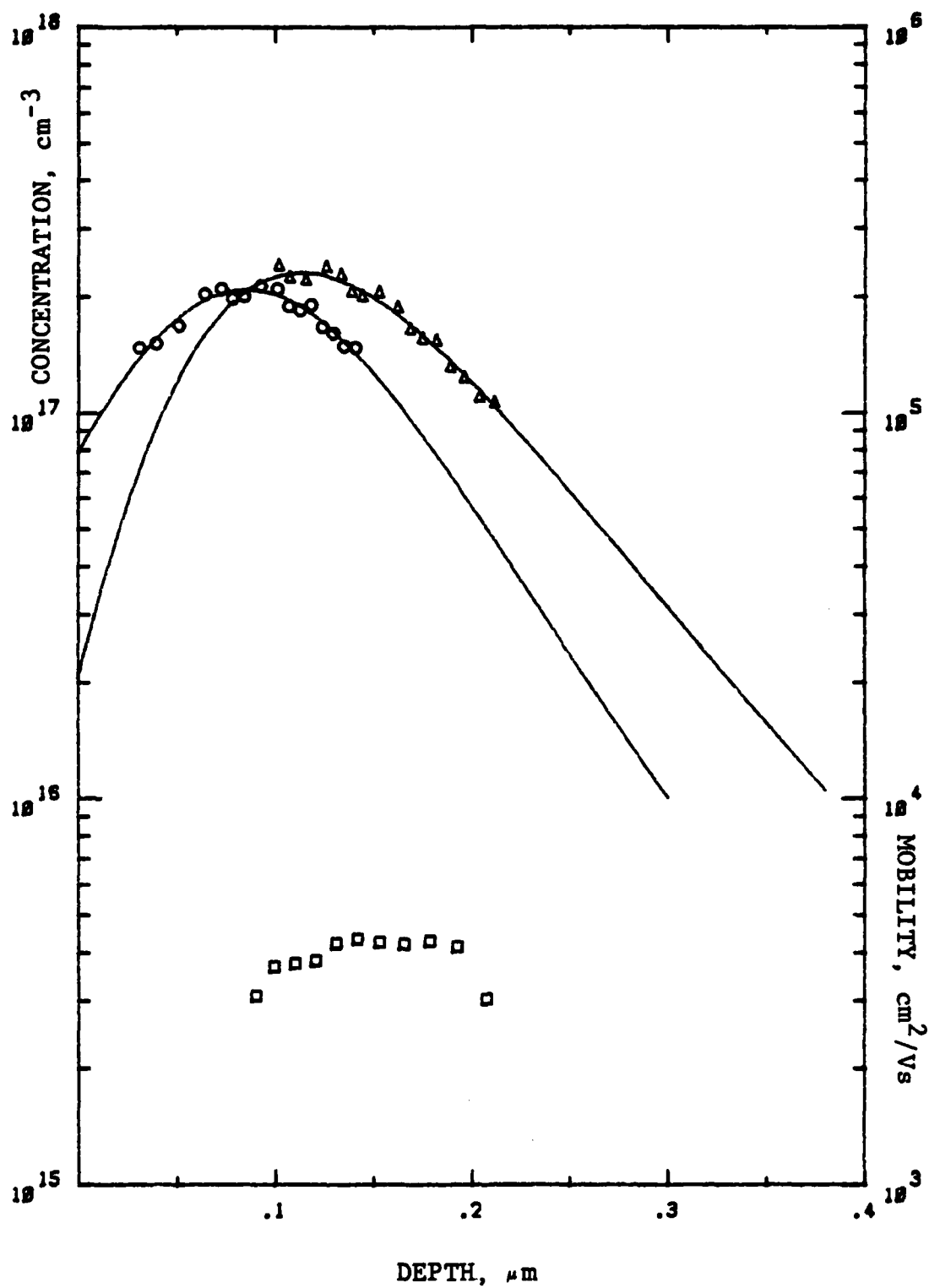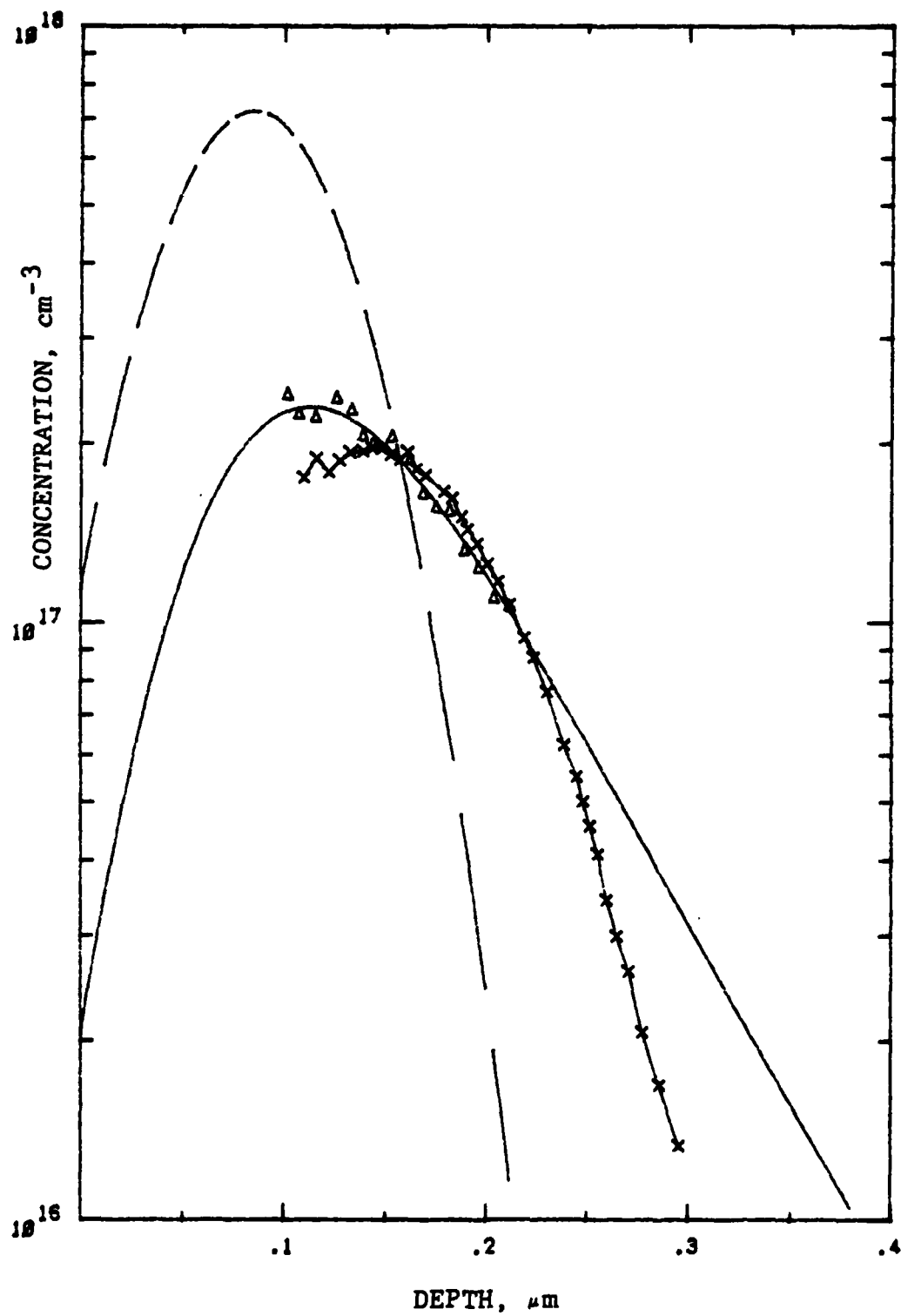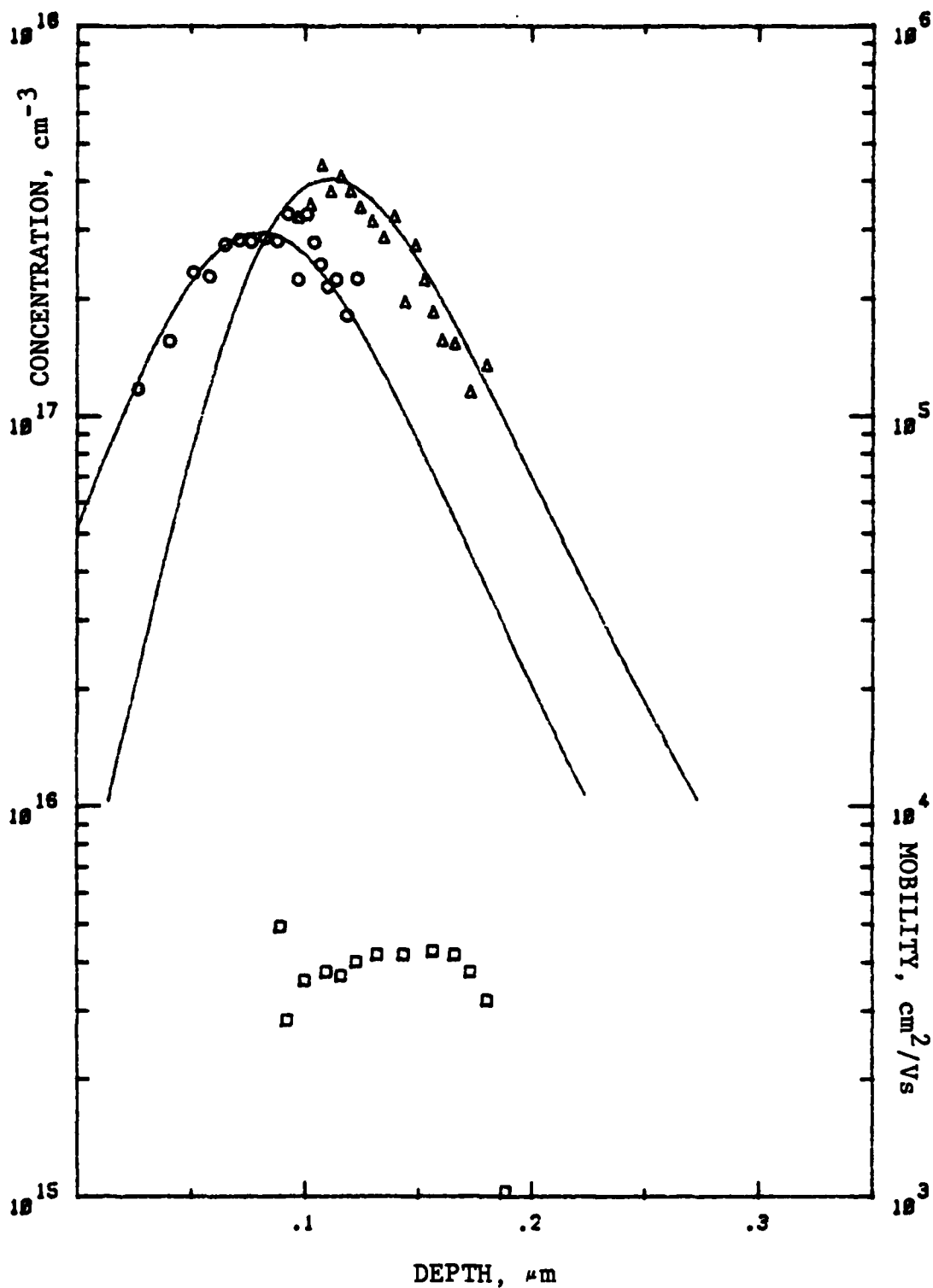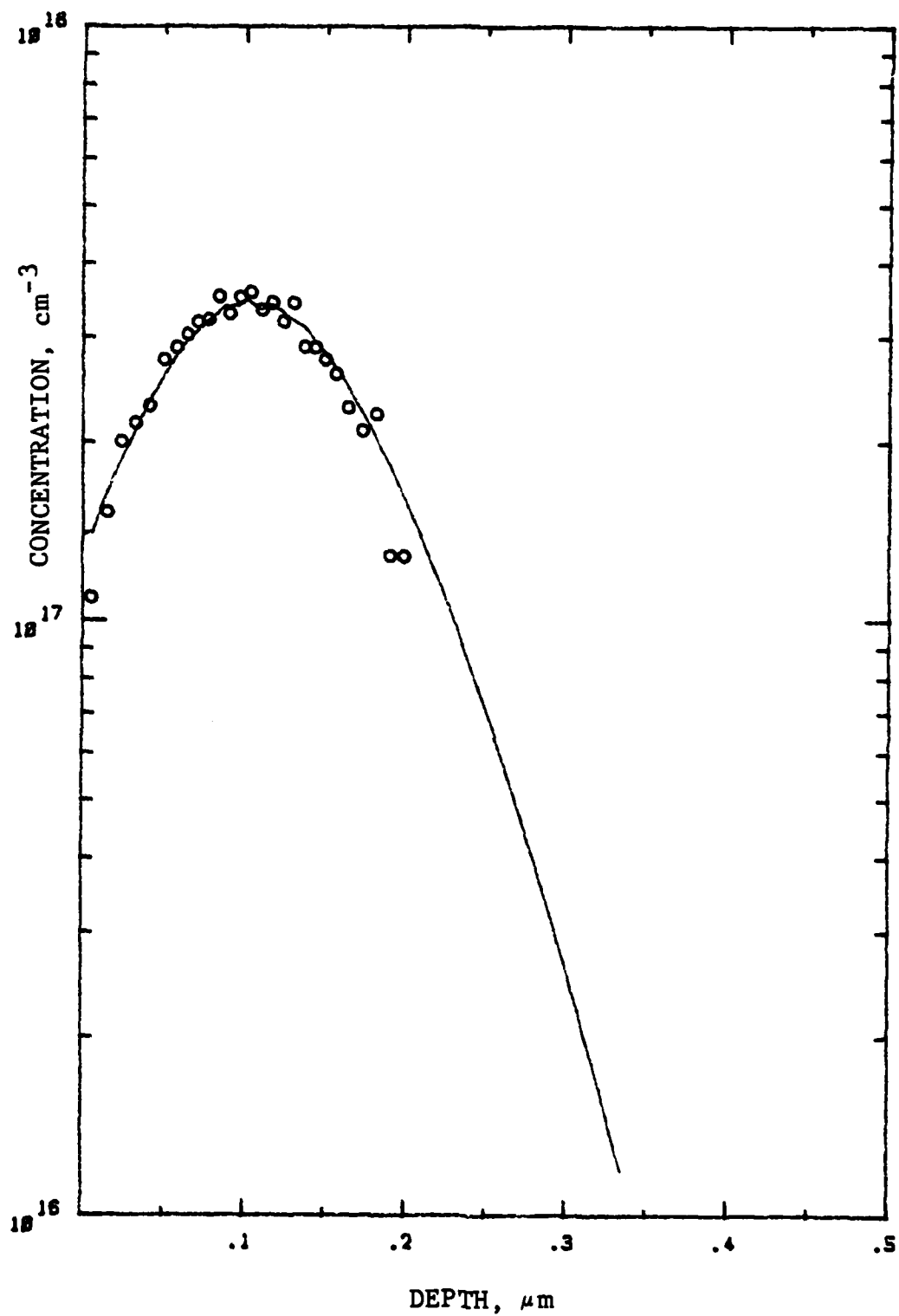Figure 19 b. 6×10^{12}: Reverse Correction

60
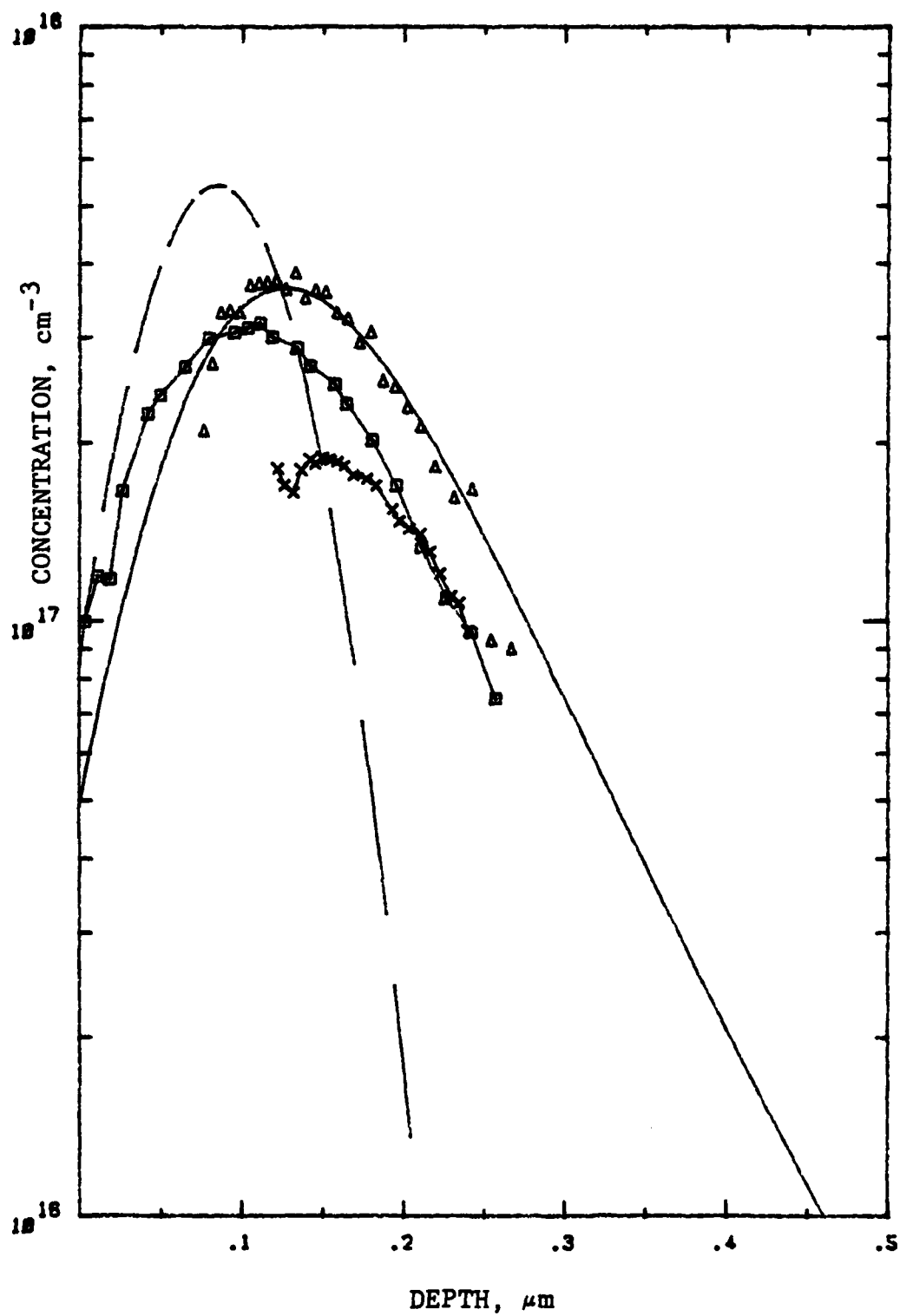
Figure 19 c. 6×10^{12}:LSS, C-V, SIMS, and Hall profiles

61

VI. CONCLUSION

The real and apparent carrier profiles have been shown to be related by the differential expression (18) and so if the depletion width is known as a function of depth the problem is immediately solved. However, if only the apparent profile is known, there is no direct way of finding the depletion widths, or the real profile. The method undertaken here has been to assume a reasonable distribution as a first guess, and to calculate from it a set of depletion widths. These depletion widths are used in conjunction with the measured profile in equation (17) to find an updated or next approximation to the real profile. It has been found that by iterating this process, the real profile attains a stable configuration, and no longer changes. This means that the real profile is consistent with the measured profile through equation (17). Thus we have found the real profile and its associated depletion widths. Correction of measured profiles has been found to take approximately 7 iterations. This extra effort is worth while since it takes several hours to gather a Hall profile.

It was comforting to find that the corrected Hall profiles were much closer to the C-V profiles than were the original measured Hall profiles, thus giving an experimental verification of the correction procedure. It

was also observed that the C-V profiles were always much smaller in peak concentration than the corrected Hall profiles. This is possibly due to conduction through the barrier at these peak concentrations. Finally, both the Hall and C-V profiles were found to have peak concentrations much lower and standard deviations much larger than those predicted by the LSS theory.

There are several advantages of the differential Hall method over the C-V method. For one, the Hall method works for profiling p-type materials while C-V profiling only works for n-type. Another advantage is that the Hall method also measures the mobility profiles. In addition, C-V profiling is not suitable at higher doping levels, such as 6×10^{12} cm^{-2}, since avalanch breakdown will occur. Most importantly, the real carrier profiles can be obtained right up to the surface from the measured Hall profile using the correction method described here. However, the C-V profiles can be obtained only beyond the original depletion width. These advantages make differential Hall profiling an important alternative to the simpler and faster C-V profiling and necessitate the use of the above procedure to correct the measured Hall profile.

APPENDIX A

PEARSON TYPE-IV DISTRIBUTION FUNCTION

The four constants a, $b_\emptyset$, b_1, b_2, of the differential equation (3) are defined in terms of the four moments of the distribution:

$$R_p = \int_{-\infty}^{\infty} x f(x)\, dx$$

$$\sigma_p^2 = \int_{-\infty}^{\infty} (x-R_p)^2 f(x)\, dx$$

$$\gamma \sigma_p^3 = \int_{-\infty}^{\infty} (x-R_p)^3 f(x)\, dx$$

$$\beta \sigma_p^4 = \int_{-\infty}^{\infty} (x-R_p)^4 f(x)\, dx$$

Where R_p is the projected range, σ_p is the standard deviation, γ is the skewness, and β is the kurtosis. In terms of these, the four constants become:

$$a = -\frac{\gamma \sigma_p (\beta + 3)}{A} = b_1$$

$$b_0 = -\frac{\sigma_p^2 (4\beta - 3\gamma^2)}{A}$$

$$b_2 = -\frac{(2\beta - 3\gamma^2 - 6)}{A}$$

where

$$A = 10\beta - 12\gamma^2 - 18.$$

Equation (3) may now be integrated to obtain an analitic function, in terms of these constants. This function is listed in line 180 of the program in appendix B.

The effect of these parameters on the distribution is demonstrated in the following graphs, where only one parameter is varied at a time. The default values are a=1, N_{max}=80000, σ_p=0.2, γ=0, and β=10. The effect of kurtosis is not demonstrated since it is very small.

APPENDIX B
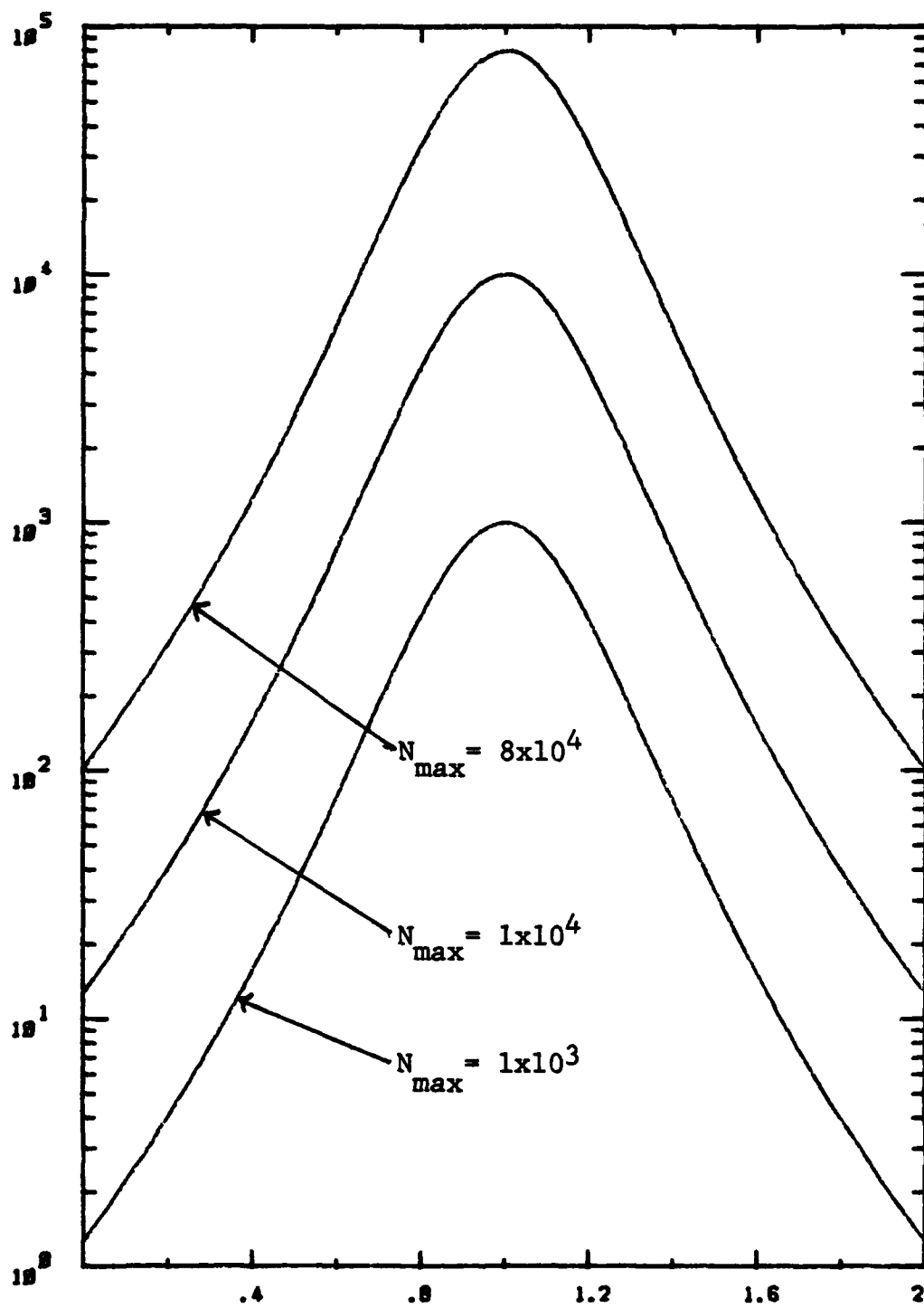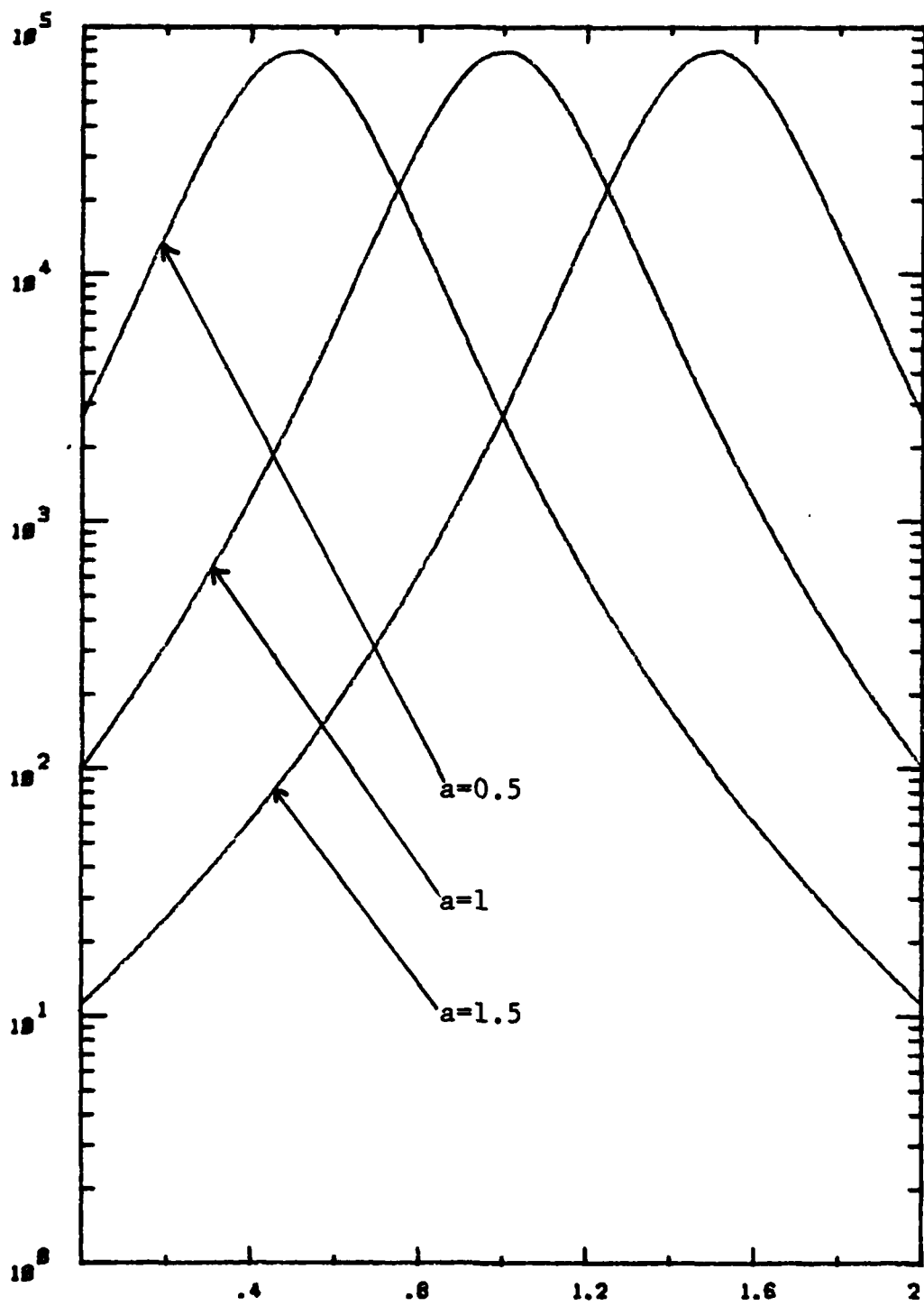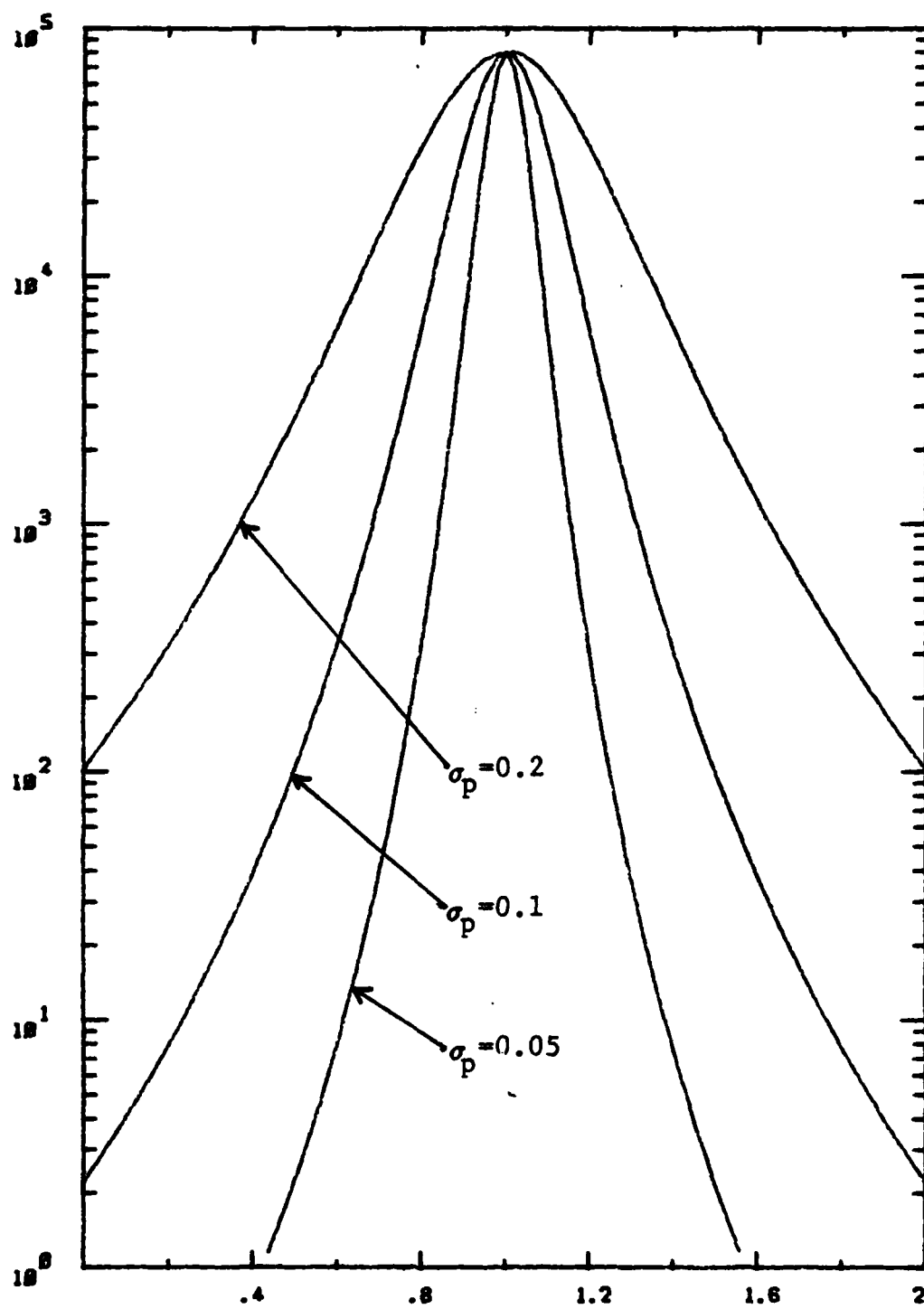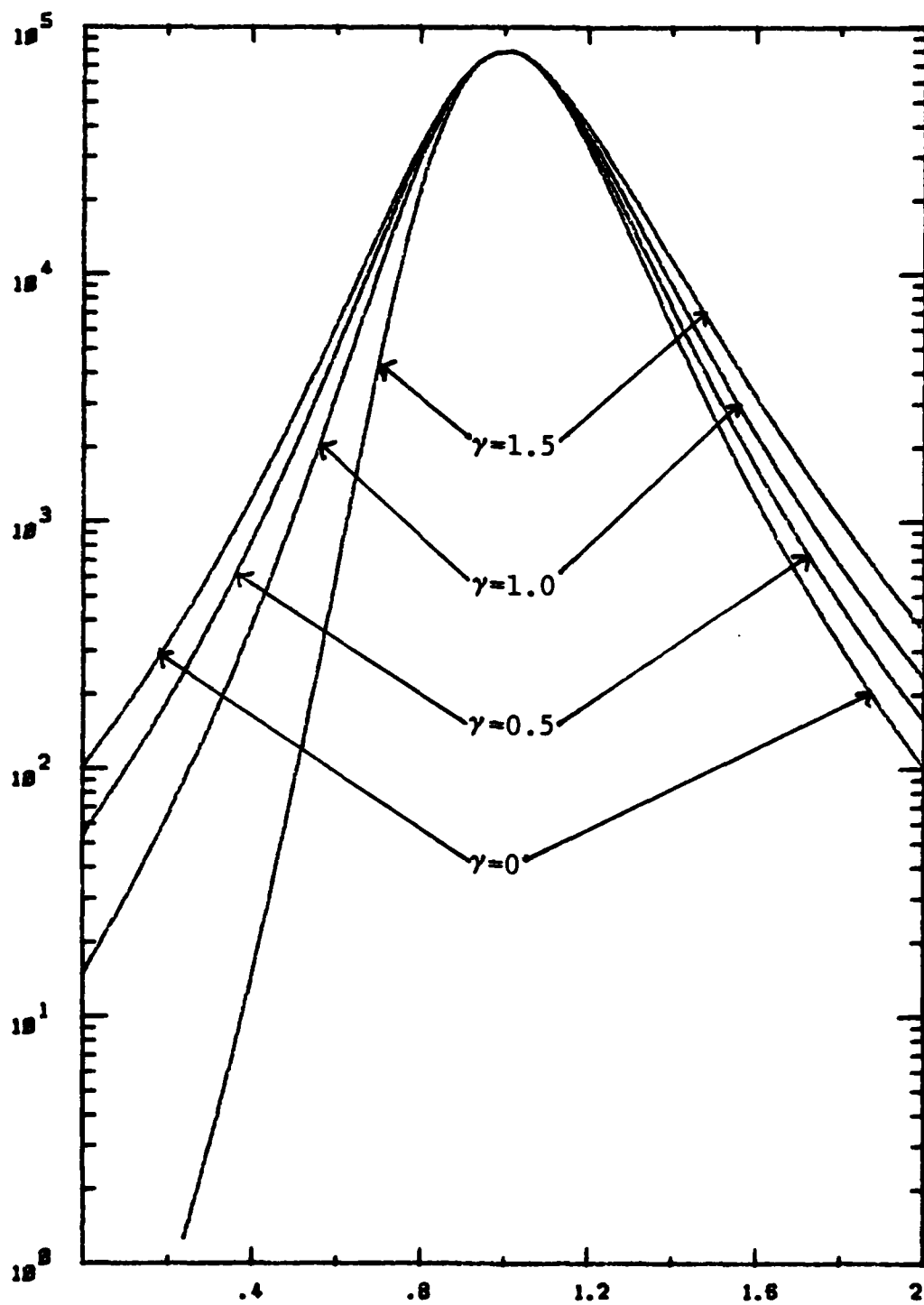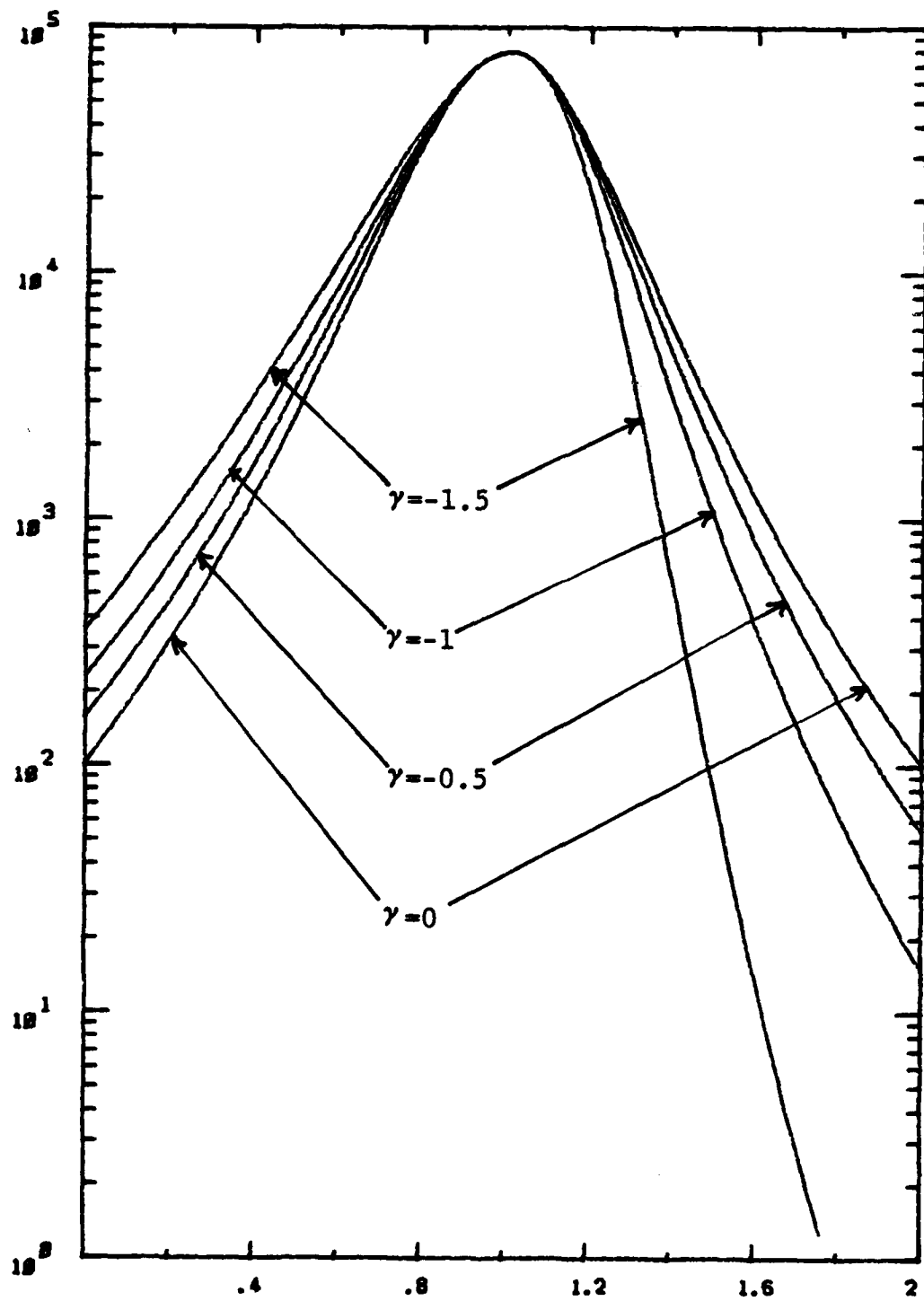
```
 1 '                          DWCORR
 2 '      from
 3 '      p.vi                                        DAVID W. ELSAESSER
 4 '      A BASIC        is included which            1 SEPT 1985
 5 '      THIS PROGRAM CORRECTS A MEASURED HALL PROFILE BY FINDING    Key words:
 6 '        AN APPROPRIATE AND SELF-CONSISTENT SET OF DEPLETION WIDTHS.
 7 '            Hall effect.
 8 '
 9 '
10 '
11 '
12 '
20 DIM
X(100),Y(100),XE(100),TI(100),NS(100).NST(100).NM(100).XM(100),XR(100),NR(1
00),XRF(100),NRF(100),NSM(100),NMP(100),MX(30),MOB(30),WM(30)
 25 DIM W(100),WF(100),NSC(500).DI(100),F(10),CX(100),CN(100)
 30 CLS:CLOSE:LT=LOG(10):CORR=0:REVCORR=0
 40 OPEN"COM1:4800,E,7,1" AS #1
 50 PRINT #1,";: "
 53 DEF FNVBS(N)=.6-.0259*LOG(4.352E+17/N)
 57 DEF FNW(N)=3.8051E+07*((VBS-.0259)/N)^.5
 60 AA=0
 70 GOSUB 2000
 85 DEF FNV(Y)=FIX(7400*(Y-CC)/YR)
 90 DEF FNH(X)=FIX(5000*(X-AA)/XR)
 95 GOSUB 1020:GOSUB 10000:GOSUB 7000
120 DEF FNA(KT,SK)=10*KT-12*SK*SK-18
130 DEF FNB0(SD,KT.SK)=-SD*SD*(4*KT-3*SK*SK)/A    'DEF CONSTANTS
140 DEF FNB1(SD,KT,SK)=-SK*SD*(KT+3)/A            'A,B0,B1,B2
150 DEF FNB2(KT.SK)=-(2*KT-3*SK*SK-6)/A
160 DEF FND(B0,B1,B2)=4*B0*B2-B1*B1
170 DEF
FNN(X)=(LOG(N0)+LOG(ABS(B0+B1*(X-XM+B1)+B2*(X-XM+B1)^2))/2/B2-ATN((2*B2*(X-
XM+B1)+B1)/DH)*(B1/B2+2*B1)/DH)/LT    'DEFINE LOG FORM OF PEAR-IV
175 DH=SQR(D)
180 DEF
FNEN(X)=N0*(ABS(B0+B1*(X-XM+B1)+B2*(X-XM+B1)^2))^(1/2/B2)*EXP(-ATN((2*B2*(X
-XM+B1)+B1)/DH)*(B1/B2+2*B1)/DH)    ' DEFINE PEAR-IV
185 INPUT "WANT TO INPUT PREVIOUS DATA: ",ANS$:IF ANS$="Y" THEN 4000 ELSE
GOSUB 7300
200 SD=.06:SK=.5:KT=10
210 GOSUB 14000
230 GOTO 260
240 INPUT "WANT TO TRY ANOTHER ITITAL SET OF PARAMETERS: ",ANS$
250 IF ANS$="N" THEN 440
260 PRINT "STANDARD DEVIATION: ":SD
270 PRINT "KURTOSIS: ":KT
280 PRINT "SKEWNESS: ":SK
290 PRINT "PEAK POSITION: ":XM
300 PRINT "MAX IN CONCENTRATION: ":NM
310 INPUT "NEW STAND. DEV.: ",TSD:IF TSD<>0 THEN SD=TSD
320 INPUT "NEW KURTOSIS: ",TKT:IF TKT<>0 THEN KT=TKT
330 INPUT "NEW SKEWNESS: ",TSK:IF TSK<>0 THEN SK=TSK
```

71

```
340 INPUT "NEW PEAK POSITION: ".TXM:IF TXM<>0 THEN XM=TXM
350 INPUT "NEW MAX IN CONCENTRATION: ",TNM:IF TNM<>0 THEN NM=TNM
360 INPUT "REPLOT AXES (NO=0, YES=1) : ",COD1:INPUT "PRINT PARAMETERS(NO=0,
YES=1)  ",COD2
370 GOSUB 14000
390 IF COD1=0 THEN 410
400 GOSUB 1000:GOSUB 7200
410 IF COD2=1 THEN GOSUB 3000
415 COD1=0:COD2=0
420 GOSUB 5000
430 GOTO 240
440 GOSUB 16020
450 SD0=SD:KT0=KT:SK0=SK:SDB=SD:KTB=KT:SKB=SK:XMB=XM:NMB=NM
455 VBS=FNVBS(NM):W=FNW(NM):XM=XM+W:FOR K=1 TO NE:XR(K)=XR(K)+W:NEXT
465 INPUT "ARE YOU FINISHED CORRECTING: ",ANS$:IF ANS$="Y" THEN 20000
470 GOSUB 13450:GOSUB 15000
475 GOTO 465
1000 '
1001 '
1002 '
1003 '                          DRAW AXES, PUT LABELS ON
1004 '
1005 '
1006 '
1010 GOSUB 2000
1020 INPUT "PRINT AXES WITH PEN# : ",PEN
1030 PRINT #1," EC 1 A 1420,2000 O ";
1035 PRINT #1," P";:PRINT #1, USING "#";PEN
1040 PRINT #1," A U 0,0 D R 5000,0 0,7400 -5000,0 0,-7400 5000,0 0,7400
-5000,0 0,-7400";
1060 PRINT #1,"A 0,0 "
1140 '
1141 '
1142 '                  DRAW Y TICS ON CONCENTRATION AXIS
1143 '
1145 '
1146 '
1150 C1=FIX(CCC):D1=FIX(DDC+.1):M=0
1160 FOR J=C1 TO D1
1170 FOR K=1 TO 9
1180 Y=LOG(K)/LT+J:L=FNV(Y)
1190 IF Y<(CCC-.05) THEN 1250
1200 IF Y>(DDC+.05) THEN 1300
1210 IF K=1 THEN 1240
1220 PRINT #1,"A ";M;",";L;"D R 75,0 -75,0 U";
1230 GOTO 1250
1240 PRINT #1,"A ";M;",";L;"D R 150,0 -150,0 U -500,-100 S13+";STR$(10);"_
";" -50,100 ";"S13+";STR$(J);"_ ";
1250 NEXT K
1260 NEXT J
1300 ' NOW DRAW TICS ON OTHER SIDE
1310 YR=YRM:DD=DDM:CC=CCM
1350 CM1=FIX(CCM+.05):DM1=FIX(DDM+.1):M=5000
1360 FOR J=CM1 TO DM1
1365 PRINT J
1370 FOR K=1 TO 9
```

72

```
1375 PRINT K
1380 Y=LOG(K)/LT+J:L=FNV(Y)
1390 IF Y<(CCM-.05) THEN 1450
1400 IF Y>(DDM+.05) THEN 1470
1410 IF K=1 THEN 1440
1420 PRINT #1,"A ";M;",";L;"D R -75,0 75,0 U";
1430 GOTO 1450
1440 PRINT #1,"A ";M;",";L;"D R -150,0 150,0 ";:IF COD3=0 THEN 1450 ELSE
PRINT #1," U 50,-100 S13+";STR$(10);"_ ";" -50,100 ";"S13+";STR$(J);"_ ";
1450 NEXT K
1460 NEXT J
1470 YR=YRC:CC=CCC:DD=DDC
1480 PRINT #1," U"
1500 '
1501 '
1502 '
1503 '          DRAW X TICS ON DEPTH AXIS
1504 '
1505 '          FIRST ON THE BOTTOM
1506 '
1520 L=0:TEST=0
1530 FOR X=.05 TO BB+.025 STEP .05
1540 M=FNH(X)
1550 IF TEST=1 THEN 1580 'GOTO BIG TIC MARK
1560 PRINT #1,"A ";M;",";L;"D R 0,50 0,-50 U";:TEST=1   'SMALL TIC MARK
1570 GOTO 1590
1580 X=FIX(10*X)/10:PRINT #1,"A ";M;",";L;"D R 0,100 0,-100 U -150,-200
S13+";STR$(X);"_ ";:TEST=0
1590 NEXT
1595 PRINT #1, "A 10000,10000 ";
1720 L=7400:TEST=0         'NOW PLOT TICS ON TOP
1730 FOR X=.05 TO BB+.025 STEP .05
1740 M=FNH(X)
1750 IF TEST=1 THEN 1780 'GOTO BIG TIC MARK
1760 PRINT #1,"A ";M;",";L;"D R 0,-50 0,50 U";:TEST=1   'SMALL TIC MARK
1770 GOTO 1790
1780 PRINT #1,"A ";M;",";L;"D R 0,-100 0,100 U ";:TEST=0
1790 NEXT
1795 PRINT #1, "A 10000,10000 ";
1800 RETURN
2000 '
2001 '
2002 '
2003 '          INPUT THE PLOTTER PARAMETERS
2004 '
2005 '
2010 INPUT "MAX IN DEPTH: ".TBB:IF TBB<>0 THEN BB=TBB
2020 INPUT "MIN IN CONCENTRATION: ",TC:IF TC<>0 THEN CCC=LOG(TC)/LT
2030 INPUT "MAX IN CONCENTRATION: ".TD:IF TD<>0 THEN DDC=LOG(TD)/LT
2035 INPUT "MIN IN CONCENTRATION PLOTTING: ",TMP: IF TMP<>0 THEN
MP=LOG(TMP)/LT
2040 INPUT "MIN IN MOBILITY: ",TCCM:IF TCCM<>0 THEN CCM=LOG(TCCM)/LT
2050 INPUT "MAX IN MOBILITY: ".TDDM:IF TDDM<>0 THEN DDM=LOG(TDDM)/LT
2060 INPUT "WANT TO PUT MOBILITY SCALE ON (1=YES, 0=NO): ",COD3
2080 XR=(BB-AA):YRC=(DDC-CCC):YRM=(DDM-CCM):YR=YRC:CC=CCC:DD=DDC
2090 IF ABS(YRC-YRM)>.001 THEN 2010
```

73

```
2100 RETURN
3000 '
3001 '
3002 '
3003 '
3004 '          PRINT   THE PEARSON 1V PARAMETERS
3005 '
3006 '
3007 '
3008 '
3009 '
3010 INPUT "PRINT PARAMETERS WITH PEN# : ",PEN:PRINT #1," P";:PRINT #1,
USING "#";PEN
3020 PRINT #1, "A 8000,5600   S14 X MAX= ";STR$(XM);"_ ";
3030 PRINT #1, "A 8000,5400   S14 N MAX= ";STR$(NM);"_ ";
3040 PRINT #1, "A 8000,5200   S14 STAND. DEV.= ";STR$(SD);"_ ";
3050 PRINT #1, "A 8000,5000   S14 SKEWNESS= ";STR$(SK);"_ ";
3060 PRINT #1, "A 8000,4800   S14 KURTOSIS= ";STR$(KT);"_ ";
3080 RETURN
4000 '
4001 '
4002 '
4003 '           INPUT EXISTING DATA
4010 FILN2$=FILN$+".DWC":FILN3$=FILN$+".COP":Z=0:COP=1
4020 OPEN "I",3,FILN2$:OPEN "O",2,FILN3$
4030 INPUT #3, NE,XM,NM,SD0,SK0,KT0
4040 FOR J=1 TO NE:INPUT #3,XR(J),NR(J):NEXT J
4050 IF EOF(3) THEN 4100
4055 PRINT XM,NM,SD0,SK0,KT0:INPUT "GO FROM HERE: ",ANS$:IF ANS$="Y" THEN
4100
4060 PRINT #2,NE,XM,NM,SD0,SK0,KT0
4070 FOR J=1 TO NE:PRINT #2,XR(J),NR(J):NEXT
4080 IF Z=0 THEN XMB=XM:NMB=NM:SDB=SD0:SKB=SK0:KTB=KT0
4090 Z=Z+1:GOTO 4030
4100 CLOSE 3:KILL FILN2$
4120 CORR=Z
4130 INPUT "ARE YOU FINISHED CORRECTING: ",ANS$:IF ANS$="Y" THEN 4140
4135 IF Z=0 THEN 240 ELSE 468
4140 PRINT #2,NE,XM,NM,SD0,SK0,KT0:FOR J=1 TO NE:PRINT #2,XR(J),NR(J):NEXT
4150 GOTO 20000
5000 REM
5005 INPUT "PLOT PEAR4 WITH PEN# : ",PEN:PRINT #1," P";:PRINT #1, USING
"#";PEN
5010 Y=FNN(AA):M=FNH(AA):L=FNV(Y):IF Y<MP THEN 5030
5020 PRINT #1,"U A ";M;",";L;" D ";
5030 DX=XR/100
5035 IF PEN=0 THEN RETURN
5040 FOR X=AA TO BB STEP DX
5050 M=FNH(X):Y=FNN(X):L=FNV(Y):IF Y<=MP THEN PRINT #1, " U ";:GOTO 5060
5055 PRINT #1,M;" ";L;" D";;
5060 NEXT
5070 PRINT #1,"U 10000,10000 ";
5100 RETURN
7000 REM
7001 REM   CALCULATE THE PROFILE
7002 REM
```

74

```
7003 REM
7010 INPUT "INPUT THE FILENAME CONTAINING HALL PROFILE DATA:
",FILN$:FILN1$=FILN$+".DAT"
7030 OPEN "I",2,FILN1$
7040 INPUT #2,I,RAT
7045 TT=0:XE(0)=0
7050 FOR K=1 TO I
7060 INPUT
#2,TI(K),NM(K):TT=TT+TI(K):XE(K)=TT*RAT/10000:DI(K)=TI(K)*RAT/10000
7080 NEXT
7085 CLOSE #2
7087 NM=0
7090 FOR K=1 TO I
7100 XM(K)=(XE(K)+XE(K-1))/2
7105 NR(K)=NM(K):XR(K)=XM(K):IF NR(K)>NM THEN NM=NR(K):XM=XR(K)
7110 NEXT K
7120 NE=I
7130 OPEN "I",2,FILN$+".MOB"
7135 INPUT #2, IM
7140 TOTM=0:MX(0)=0
7145 FOR K=1 TO IM
7150 INPUT #2,X,MOB(K):TOTM=TOTM+X:MX(K)=TOTM*RAT/10000
7155 NEXT
7160 CLOSE #2
7200 REM   PLOT THIS DATA
7202 INPUT "PLOT DATA WITH PEN# : ",PEN:PRINT #1," P";:PRINT #1, USING
"#";PEN;
7210 FOR K=1 TO I
7215 IF NM(K)<0 THEN 7240
7220 X=FNH(XM(K)):Y=LOG(NM(K))/LT:IF Y<MP THEN 7240 ELSE Y=FNV(Y)
7225 IF X>5000 THEN 7240
7230 PRINT #1, "CC ";X;",";Y;"35";
7240 NEXT
7250 PRINT #1, " U A 10000,10000";
7260 RETURN
7300 REM
7310 FILN2$=FILN$+".DWC"
7320 OPEN "O",2,FILN2$
7400 RETURN
7500 REM   PLOT THIS DATA USING TRIANGLES
7502 INPUT "PLOT DATA WITH PEN# : ",PEN:PRINT #1," P";:PRINT #1. USING
"#";PEN;
7510 FOR K=1 TO NE
7515 IF NR(K)<0 THEN 7540
7520 X=FNH(XR(K)):Y=LOG(NR(K))/LT:IF Y<MP THEN 7540 ELSE Y=FNV(Y)
7525 IF X>5000 THEN 7540
7530 PRINT #1, X;",";Y;" M44 ";
7540 NEXT
7550 PRINT #1, " U A 10000,10000";
7560 RETURN
7600 REM
7610 FILN2$=FILN$+".DWC"
7620 OPEN "O",2,FILN2$
7700 RETURN
8000 '
8001 '
```

75

```
8002 '    CALCULATE THE CORRECTED PROFILE
8003 '          FIND DEPLETION WIDTHS
8004 '
8005 '
8010 '   COMPUTE SHEET CONCENTRATIONS
8020 PRINT "INTEGRATING N(X)"
8040 INPUT "XMAX FOR INTEGRATION: ",XMAX
8050 H0=XMAX/500
8055 NSC(0)=0
8060 FOR J=1 TO 500
8070 F1=FNEN((J-.5)*H0):NSC(J)=NSC(J-1)+F1*H0/10000
8075 PRINT J,NSC(J)
8090 NEXT
8095 H1=(XMAX-.1)/100
8100 INPUT "W0: ",W(0)
8110 FOR J=0 TO 100
8115 Z=0
8120 IF J<>0 THEN W(J)=W(J-1)
8130 X=(W(J)+J*H1)/H0:K=FIX(X):DK=X-K:Y=J*H1/H0:L=FIX(Y):DL=Y-L
8140 IF X>500 THEN NE=J-1:GOTO 8230
8150 N=(NSC(K)+(NSC(K+1)-NSC(K))*DK-NSC(L)-(NSC(L+1)-NSC(L))*DL)*10000/W(J)
8160 VBS=FNVBS(N):WF=FNW(N)
8165 Z=Z+1:IF Z>50 THEN INPUT "WF: ",WF:Z=1
8170 IF ABS(W(J)-WF)<.0001 THEN 8210
8180 W(J)=(W(J)+WF)/2
8200 GOTO 8130
8210 PRINT J,W(J)
8220 NEXT
8225 NE=100
8230 IF REVCORR=1 THEN RETURN
8235 GOSUB 9000
8300 REM CORRECT THIS PROFILE
8310 TNM=0
8315 PRINT NE
8320 FOR J=1 TO NE
8340 XR(J)=((2*J-1)*H1+W(J)+W(J-1))/2
8350 NR(J)=NMP(J)/(1+(W(J)-W(J-1))/H1)
8360 IF NR(J)>TNM THEN TNM=NR(J):TXM=XR(J)
8365 PRINT J,XR(J),NR(J)
8370 NEXT
8500 REM  PLOT THE CORRECTED CURVE
8510 INPUT "PLOT DATA WITH PEN# : ",PEN:PRINT #1," P";:PRINT #1, USING
"#";PEN;
8515 IF NR(1)<0 THEN NR(1)=1E+15
8520 X=FNH(XR(1)):Y=LOG(NR(1))/LT:IF Y<MP THEN 8530 ELSE Y=FNV(Y)
8525 PRINT #1, "U ";X;",";Y;"D ";
8530 FOR K=2 TO NE
8540 IF NR(K)<0 THEN 8570
8550 X=FNH(XR(K)):Y=FNV(LOG(NR(K))/LT)
8555 IF X=>5000 THEN 8570
8560 PRINT #1, X;",";Y;
8565 IF Y<=0 THEN PRINT #1, " U "; ELSE PRINT #1, " D ";
8570 NEXT
8580 PRINT #1, " U A 10000,10000 ";
8590 RETURN
9000 '
```

```
9020 FOR J=1 TO NE
9030 X=((2*J-1)*H1+W(J)+W(J-1))/2:NMP(J)=FNEN(X)*(1+(W(J)-W(J-1))/H1)
9040 NEXT
9050 XM=XMB:NM=NMB:SD=SDB:SK=SKB:KT=KTB:GOSUB 14000
9070 FOR J=1 TO NE
9080 NMP(J)=(FNEN((J-.5)*H1)+NMP(J))/2
9090 NEXT
9100 RETURN
10000 REM INPUT C-V FILE
10050 INPUT "DOSE: ",DOSE
10060 INPUT "LSS RP: ",RP:INPUT "LSS STAN. DEV.: ",SIG
10070 NG=DOSE*10000/SIG/2.5066283#:DEF FNLSS(X)=NG*EXP(-((X-RP)/SIG)^2/2)
10075 INPUT "BEGINNING MEASURED SHEET CONCENTRATION: ",NSMO
10080 PRINT "MAX IN LSS: ",NG
10100 INPUT "NAME OF C-V FILE: ",CFILN$:CFILN$=CFILN$+".DAT"
10110 OPEN "I",4,CFILN$
10120 INPUT #4,CN
10130 FOR J=1 TO CN:INPUT #4,CX(J),CN(J):NEXT
10140 CLOSE 4
10200 RETURN
10250 '
10255 INPUT "PLOT C-V DATA WITH PEN# : ",PEN:PRINT #1," P";:PRINT #1, USING
"#";PEN;
10260 L=FNH(CX(1)):Y=LOG(CN(1))/LT:M=FNV(Y):IF Y<MP THEN 10270 ELSE PRINT
#1,"U ";L;",";M;"D ";
10270 FOR J=1 TO CN
10280 L=FNH(CX(J)):Y=LOG(CN(J))/LT:M=FNV(Y):IF Y<MP THEN 10300
10285 IF X>5000 THEN 10300
10290 PRINT #1,L;",";M;", M41 "
10300 NEXT
10310 PRINT #1,"U 10000,10000"
10400 RETURN
10500 '                PLOTT LSS FUNCTION
10520 DX=XR/100
10530 INPUT "PLOT LSS WITH PEN#: ",PEN:PRINT #1," P";:PRINT #1, USING
"#";PEN;
10540 L=FNH(0):M=FNV(LOG(FNLSS(0))/LT):PRINT #1," U ";L;",";M;"D ";:Z=0
10550 FOR X=AA TO BB STEP DX
10560 Z=Z+1
10570 L=FNH(X):Y=LOG(FNLSS(X))/LT:M=FNV(Y)
10573 IF Y<=MP THEN PRINT #1, "U ":X=BB+1:GOTO 10600
10580 IF Z=4 THEN PRINT #1," U ";L;",";M;" D";:Z=0:GOTO 10600
10590 PRINT #1, L;",";M;
10600 NEXT
10650 PRINT #1," U 10000,10000";
10660 RETURN
10800 '            PLOTT THE CORRECTED MOBILITIES
10805 INPUT "PLOT MOBILITY WITH PEN# : ",PEN:PRINT #1," P";:PRINT #1, USING
"#";PEN;
10810 CC=CCM:DD=DDM:YR=YRM
10820 FOR J=1 TO NEM
10830 X=(MX(J)+MX(J-1)+WM(J)+WM(J-1))/2:X=FNH(X)
10835 IF MOB(J)<=0 THEN 10870
10840 Y=LOG(MOB(J))/LT
10850 IF Y<CCM OR Y>CCM+1 THEN 10870
10855 IF X>5000 THEN 10870
```

```
10860 Y=FNV(Y):PRINT #1, X;",";Y;" M42";
10870 NEXT
10880 CC=CCC:DD=DDC:YR=YRC
10900 RETURN
11000 '
11100 INPUT "NAME OF DATA FILE: ",CFILN$:CFILN$=CFILN$+".DAT"
11110 OPEN "I",4,CFILN$
11120 INPUT #4,CN
11130 FOR J=1 TO CN:INPUT #4,X(J),Y(J):NEXT
11140 CLOSE 4
11255 INPUT "PLOT PROFILE WITH PEN# : ",PEN:PRINT #1," P";:PRINT #1, USING
"#";PEN;
11260 L=FNH(X(1)):Y=LOG(Y(1))/LT:M=FNV(Y):IF Y<MP THEN 11270 ELSE PRINT
#1,"U ";L;",";M;"D ";
11270 FOR J=1 TO CN
11280 L=FNH(X(J)):Y=LOG(Y(J))/LT:M=FNV(Y):IF Y<MP THEN 11300
11285 IF L>5000 THEN 11300
11290 PRINT #1,L;",";M;", M42 "
11300 NEXT
11310 PRINT #1,"U 10000,10000"
11400 RETURN
13450 REM
13480 PRINT "STANDARD DEVIATION: ";SD0
13490 PRINT "KURTOSIS: ";KT0
13500 PRINT "SKEWNESS: ";SK0
13510 PRINT "PEAK POSITION: ";XM
13520 PRINT "MAX IN CONCENTRATION: ";NM
13530 INPUT "NEW STAND. DEV.: ",TSD:IF TSD<>0 THEN SD0=TSD
13540 INPUT "NEW KURTOSIS: ",TKT:IF TKT<>0 THEN KT0=TKT
13550 INPUT "NEW SKEWNESS: ",TSK:IF TSK<>0 THEN SK0=TSK
13560 INPUT "NEW PEAK POSITION: ",TXM:IF TXM<>0 THEN XM=TXM
13570 INPUT "NEW MAX IN CONCENTRATION: ",TNM:IF TNM<>0 THEN NM=TNM
13580 INPUT "REPLOT AXES (0=NO, YES=1) : ",COD1:INPUT "PRINT PARAMETERS
(NO=0, YES=1) : ",COD2
13590 INPUT "CLEAR: ",CL:IF CL=1 THEN PRINT #1,"Z ;:";
13600 IF COD1=0 THEN 13620
13610 GOSUB 1000:GOSUB 8500
13620 SD=SD0:KT=KT0:SK=SK0:GOSUB 14000
13625 IF COD2=1 THEN GOSUB 3000:COD2=0
13630 SD0=SD:KT0=KT:SK0=SK
13640 RETURN
14000 REM
14020
A=FNA(KT,SK):B0=FNB0(SD,KT,SK):B1=FNB1(SD,KT,SK):B2=FNB2(KT,SK):D=FND(B0,B1
,B2)
14080 IF D<=0 THEN PRINT "DISCRIMINANT = ";D:GOTO 14100
14090 GOTO 14250
14100 REM
14110 PRINT "INPUT NEW PARAMETERS "
14120 PRINT "STANDARD DEVIATION: ";SD
14130 PRINT "KURTOSIS: ";KT
14140 PRINT "SKEWNESS: ";SK
14150 PRINT "PEAK POSITION: ";XM
14160 PRINT "MAX IN CONCENTRATION: ";NM
14170 INPUT "NEW STAND. DEV.: ",TSD:IF TSD<>0 THEN SD=TSD
14180 INPUT "NEW KURTOSIS: ",TKT:IF TKT<>0 THEN KT=TKT
```

```
14190 INPUT "NEW SKEWNESS: ".TSK:IF TSK<>0 THEN SK=TSK
14200 INPUT "NEW PEAK POSITION: ",TXM:IF TXM<>0 THEN XM=TXM
14210 INPUT "NEW MAX IN CONCENTRATION: ",TNM:IF TNM<>0 THEN NM=TNM
14220 GOTO 14020
14250 DH=SQR(D):NO=1:HO=NM/FNEN(XM)
14260 RETURN
15000 '
15100 '
15110 PRINT "CHANGE PAPER ":GOSUB 5000
15120 INPUT "DO YOU WANT TO CORRECT NOW: ",ANS$
15130 IF ANS$="Y" THEN GOSUB 16000 ELSE RETURN
15132 TTXM=XM:TTNM=NM
15135 GOSUB 8000
15137 INPUT "WANT TO PLOT REVCORRECTED DATA: ",ANS$:IF ANS$="Y" THEN GOSUB
17000
15138 XM=TXM:NM=TNM
15140 GOSUB 1000:GOSUB 8500:GOSUB 10250
15150 INPUT "CHANGE PAPER THEN RETURN: ",ANS$
15160 INPUT "WANT TO PLOT REVCORRECTED DATA: ",ANS$:IF ANS$="Y" THEN GOSUB
17000
15300 RETURN
16000 REM
16010 SD=SD0:SK=SK0:KT=KT0:CORR=CORR+1
16020 LPRINT "CORRECTION #";CORR
16030 LPRINT "XMAX: ";XM
16040 LPRINT "NMAX: ";NM
16050 LPRINT "STANDARD DEVIATION: ";SD
16060 LPRINT "SKEWNESS: ";SK
16070 LPRINT "KURTOSIS: ";KT:LPRINT:LPRINT
16080 PRINT #2,NE,XM,NM,SD,SK,KT
16090 FOR J=1 TO NE:PRINT #2,XR(J),NR(J):NEXT
16100 RETURN
17000 '
17100 '     CALCULATE THE REVERSE CORRECTED MEASURED DATA
17110 INPUT "CHANGE PAPER, THEN RETURN:",ANS$
17120 GOSUB 1000
17140 PRINT "NOW PLOTTING ORIGINAL MEASURED DATA
":XM=XMB:NM=NMB:SD=SDB:SK=SKB:KT=KTB:GOSUB 1400:GOSUB 5000
17145 NM=TTNM:XM=TTXM:SD=SD0:KT=KT0:SK=SK0:GOSUB 14000:FOR J=1 TO
NE:X(J)=XR(J):Y(J)=NR(J):NEXT
17150 FOR J=1 TO
NE:X=((2*J-1)*H1+(W(J)+W(J-1)))/2:NR(J)=FNEN(X)*(1+(W(J)-W(J-1))/H1):XR(J)=
(J-.5)*H1:NEXT
17170 PRINT "NOW PLOTTING REVERSE CORRECTED DATA "
17180 GOSUB 8500
17190 FOR J=1 TO NE:XR(J)=X(J):NR(J)=Y(J):NEXT
17300 RETURN
20000 '
20001 '
20002 '
20003 '
20004 '
20005 '    FINISHED CORRECTING -- NOW CHECK FOR SELF CONSISTENCY
20006 '       AND PRINT FINAL PLOTS
20007 '
20008 '
```

79

```
20009 '
20010 NEL=NE:XML=XM:NML=NM:SDL=SDO:SKL=SKO:KTL=KTO
20015 FOR J=1 TO NEL:XRF(J)=XR(J):NRF(J)=NR(J):NEXT
20020 SD=SDO:SK=SKO:KT=KTO
20030 GOSUB 14000
20040 CLOSE 2:IF COP=1 THEN NAME FILN3$ AS FILN2$
20050 PRINT "INTEGRATING FOR FINAL TIME" :REVCORR=1:GOSUB 8040
20100 '    CALCULATE THE REVERSE CORRECTED MEASURED DATA
20110 INPUT "CHANGE PAPER, THEN RETURN:",ANS$
20120 GOSUB 1000
20130 FOR J=1 TO I:XR(J)=XM(J):NR(J)=NM(J):NEXT:NE=I
20140 PRINT "NOW PLOTTING ORIGINAL MEASURED DATA ":GOSUB 7200
20145 NE=NEL:XM=XML:NM=NML:SD=SDL:SK=SKL:KT=KTL:GOSUB 14000
20150 FOR J=1 TO
NE:X=((2*J-1)*H1+(W(J)+W(J-1)))/2:NR(J)=FNEN(X)*(1+(W(J)-W(J-1))/H1):XR(J)=
(J-.5)*H1:NEXT
20170 PRINT "NOW PLOTTING REVERSE CORRECTED DATA "
20180 GOSUB 8500
20300 '         CALCULATING DEPLETION WIDTHS FOR MEASURED DATA
20305 PRINT" NOW CALCULATING DEPLETION WIDTHS FOR MEASURED DATA"
20310 INPUT "W0: ",WF(0)
20320 FOR J=0 TO I
20340 Z=0
20350 IF J<>0 THEN WF(J)=WF(J-1)
20360 X=(WF(J)+XE(J))/HO:K=FIX(X):DK=X-K:Y=XE(J)/HO:L=FIX(Y):DL=Y-L
20370 IF X>500 THEN NE=J-1:GOTO 20500
20380
N=(NSC(K)+(NSC(K+1)-NSC(K))*DK-NSC(L)-(NSC(L+1)-NSC(L))*DL)*10000/WF(J)
20385 NSM(J)=NSC(K)+(NSC(K+1)-NSC(K))*DK
20390 VBS=FNVBS(N):WT=FNW(N)
20400 Z=Z+1:IF Z>50 THEN INPUT "WF: ",WT:Z=1
20410 IF ABS(WF(J)-WT)<.0001 THEN 20450
20430 WF(J)=(WF(J)+WT)/2
20440 GOTO 20360
20450 PRINT J,WF(J)
20460 NEXT
20465 NE=I
20470 GOSUB 25000
20500 '
20510 X=WF(O)/HO:K=FIX(X):DK=X-K
20540 LPRINT:LPRINT "ORIGINAL DEPLETION WIDTH: ",WF(0)
20550 LPRINT "APPARENT ACTIVATION EFFICIENCY: ";NSMO*100/DOSE
20560 LPRINT "TRUE ACTIVATION EFFICENCY:
";(NSMO+NSC(K)+(NSC(K+1)-NSC(K))*DK)*100/DOSE
20570 LPRINT "THE APPROXIMATE NUMBER OF SURFACE STATES IS:
";NSC(K)+(NSC(K+1)-NSC(K))*DK
20600 '      PLOT THE MEASURED DATA  AND  CORRECT THE MEASURED DATA
20610 PRINT "READY TO PLOT MEASURED DATA":INPUT "CHANGE PAPER,  THEN
RETURN",ANS$
20620 GOSUB 1000
20630 FOR J=1 TO I:XR(J)=XM(J):NR(J)=NM(J):NEXT
20640 GOSUB 7200
20650 FOR J=1 TO I
20660 NR(J)=NM(J)/(1+(WF(J)-WF(J-1))/DI(J)):XR(J)=XM(J)+(WF(J)+WF(J-1))/2
20670 NEXT
20675 PRINT "PLOT THE CORRECTED DATA "
```

```
20680 GOSUB 7500 'PLOT TRIANGLES FOR CORRECTED DATA
20700 '          NOW PLOT THE MEASURED AND CORRECTED PEARSON IV
20710 PRINT "PLOT THE PEARSON IV FIT TO THE ORIGINAL DATA"
20720 XM=XMB:NM=NMB:SD=SDB:SK=SKB:KT=KTB:GOSUB 14000:GOSUB 5000
20730 PRINT "PLOT THE PEARSON IV FIT TO THE CORRECTED DATA"
20740 XM=XML:NM=NML:SD=SDL:SK=SKL:KT=KTL:GOSUB 14000:GOSUB 5000
20742 INPUT "WANT TO PLOT MOBILITIES ",ANS$:IF ANS$="Y" THEN GOSUB 10800
20745 GOSUB 1000:PRINT "CORRECTED DATA ":GOSUB 7500:PRINT "CORRECTED
FIT":GOSUB 5000
20750 PRINT "NOW PLOT LSS ":GOSUB 10500
20760 PRINT "NOW PLOT C-V DATA":GOSUB 10250
20850 INPUT "DO YOU WANT PLOT ANOTHER MEASURED PROFILE: ",ANS$
20860 IF ANS$="Y" THEN GOSUB 11000
21770 INPUT "WANT TO PLOT MOBILITIES ",ANS$:IF ANS$="Y" THEN GOSUB 10800
21850 INPUT "DO YOU WANT MORE COPIES: ",ANS$
21860 IF ANS$<>"N" THEN GOTO 20110
21900 END
25000 ' CALCULATE DEPLETION WIDTHS FOR THE MOBILITY DATA
25020 PRINT:PRINT "CALCULATING DEPLETION WIDTHS FOR THE MOBILITY DATA
":PRINT
25310 INPUT "WO: ",WM(0)
25320 FOR J=0 TO IM
25340 Z=0
25350 IF J<>0 THEN WM(J)=WM(J-1)
25360 X=(WM(J)+MX(J))/HO:K=FIX(X):DK=X-K:Y=MX(J)/HO:L=FIX(Y):DL=Y-L
25370 IF X>500 THEN NEM=J-1:GOTO 25500
25380
N=(NSC(K)+(NSC(K+1)-NSC(K))*DK-NSC(L)-(NSC(L+1)-NSC(L))*DL)*10000/WM(J)
25390 VBS=FNVBS(N):WT=FNW(N)
25400 Z=Z+1:IF Z>50 THEN INPUT "WM: ",WT:Z=1
25410 IF ABS(WM(J)-WT)<.0001 THEN 25450
25430 WM(J)=(WM(J)+WT)/2
25440 GOTO 25360
25450 PRINT J,WF(J)
25460 NEXT
25465 NEM=IM
25470 RETURN
```

81

BIBLIOGRAPHY

1. Stephens, K. G. and B. J. Sealy "Use of ion implantation in future GaAs technology," Microelectronics, J.9: 13-18 (1978)

2. Dearnaley, G. et al. Ion Implantation. Amsterdam: North-Holland Publishing Company, 1973

3. Morgan, D. V. et al. "Prospects for Ion Bombardment and Ion Implantation in GaAs and InP device fabrication," IEE Proceedings, 128: 109-130 (August 1981)

4. Kim, Yong Yun. Electrical Properties of Silicon-Implanted GaAs. MS Thesis. PH-82D-17. School of Engineering, Air Force Institute of Technology (AU), Wright-Patterson AFB, OH. December 1982.

5. NASA. Charaterization of Silicon-Gate CMOS/SOS Integrated Circuits with Ion Implantation. Brief no. MFS-23995. Marshal Space Flight Center, 1977

6. Hofker W. K. Implantation of Boron in Silicon. Phillips Research Reports Supplements, Supplement 8, 1975

7. Many A. et al. Semiconductor Surfaces. Amsterdam: North-Holland Publishing Company, 1965

8. Shockley, William. "On the Surface States Associated with a Periodic Potential," Physical Review, 56: 317-323 (August 1939)

9. Massies, J. et al. "Application of Molecular Beam Epitaxy to Study the Surface Properties of III-V Compounds," Proceedings of the 3rd International Conference on Solid Surfaces 639-641. Vienna, 1977

10. Chandra, A. et al. "Surface and Interface Depletion Corrections to Free Carrier-Density Determinations by Hall Measurements," Solid State Electronics, 22: 645-650 (December 1979)

11. Pianetta, P. et al. "The Surface Structure and Surface Chemistry of GaAs (100)," Proceedings of the 3rd International Conference on Solid Surfaces 639-641. Vienna, 1977

12. Hattori K. and Y. Izumi. "The Electrical
    Characterization of degererate InP diodes with an
    Interfacial layer," Journal of applied Physics, 53:
    6906-6910 (October 1982)

13. Henisch, H. K. Rectifying Semiconductor Contacts.
    Oxford: The Clarendon Press, 1957

14. L. J. van der Pauw. "A Method of Measuring Specific
    Resistivity and Hall-Effect of Discs of Arbitrary
    Shape." Phillips Research Reports, 13: 1-9 (February
    1958)

15. Mayer, J. W. et al. "Ion Implantation of Silicon:
    Electrical Evaluation Using Hall-Effect
    Measurements,"Canadian Journal of Physics, 45:
    4073-4089 (September 1967)

16. Petritz, Richard L. "Theory of an Experiment for
    Measuring the Mobility and Density of Carriers in the
    Space-Charge Region of a Semiconductor Surface,"
    Physical Review, 110: 1254-1263 (June 1958)

17. Yeo, Y. K. et al. "Substrate-Dependent Electrical
    Properties of Low Dose Si Implants in GaAs," To be
    published in Journal of Applied Physics (December
    1985)

VITA

David William Elsaesser was born on 7 March 1962 in Cincinnati, Ohio. He graduated from high school in 1980, and then attended Xavier University in Cincinnati, from which he received the degree of Bachelor of Science in Physics. Upon graduation, he received a commission in the USAF through the ROTC program at the University of Cincinnati. His first assignment was to the Air Force Institute of technology, with a subsequent assignment to the Electronics Research Branch of the Avionics Lab, both at Wright-Patterson AFB, Ohio.

Permanent Address: 215 Anderson Ferry Rd.
Cincinnati, Ohio 45238

REPORT DOCUMENTATION PAGE

1a. REPORT SECURITY CLASSIFICATION UNCLASSIFIED	1b. RESTRICTIVE MARKINGS
2a. SECURITY CLASSIFICATION AUTHORITY	3. DISTRIBUTION/AVAILABILITY OF REPORT APPROVED FOR PUBLIC RELEASE DISTRIBUTION UNLIMITED
2b. DECLASSIFICATION/DOWNGRADING SCHEDULE	

4. PERFORMING ORGANIZATION REPORT NUMBER(S) AFIT/GEP/ENP/85D-3	5. MONITORING ORGANIZATION REPORT NUMBER(S)

6a. NAME OF PERFORMING ORGANIZATION AFIT/ENP	6b. OFFICE SYMBOL (If applicable) 255-4498	7a. NAME OF MONITORING ORGANIZATION
6c. ADDRESS (City, State and ZIP Code) Wright-Patterson AFB, Ohio 45433		7b. ADDRESS (City, State and ZIP Code)

8a. NAME OF FUNDING/SPONSORING ORGANIZATION	8b. OFFICE SYMBOL (If applicable)	9. PROCUREMENT INSTRUMENT IDENTIFICATION NUMBER

8c. ADDRESS (City, State and ZIP Code)	10. SOURCE OF FUNDING NOS.			
	PROGRAM ELEMENT NO.	PROJECT NO.	TASK NO.	WORK UNIT NO.

11. TITLE (Include Security Classification)
See item 19

12. PERSONAL AUTHOR(S)
Elsaesser, David W., Second Lieutenant, USAF

13a. TYPE OF REPORT MS Thesis	13b. TIME COVERED FROM _____ TO _____	14. DATE OF REPORT (Yr., Mo., Day) 1985 December	15. PAGE COUNT 91

16. SUPPLEMENTARY NOTATION

17. COSATI CODES			18. SUBJECT TERMS (Continue on reverse if necessary and identify by block number)
FIELD	GROUP	SUB. GR.	Surface depletion, Hall-effect, Carrier profiles Ion Implantation, van der Pauw
20	12		

19. ABSTRACT (Continue on reverse if necessary and identify by block number)

Approved for public release IAW AFR 190-1
LYNN E. WOLAVER
Dean for Research and Professional Development
Air Force Institute of Technology (AFIT)
Wright-Patterson AFB OH 45433

TITLE: SURFACE DEPLETION CORRECTION TO CARRIER PROFILES BY HALL MEASUREMENTS

A method was developed for correcting a carrier profile by Hall measurements for the surface depletion effect. The method assumes that the experimental data is to be fit with a Pearson type-IV curve.
In order to correct the measured profile it is necessary to know the depletion width after each etch. The depletion widths are dependent upon the real profile and not the measured, therefore if one only has the measured data, the depletion widths cannot be directly determined. In order to gain insight into the problem a procedure called "reverse correction" is developed. It creates a (cont.)

20. DISTRIBUTION/AVAILABILITY OF ABSTRACT UNCLASSIFIED/UNLIMITED ☒ SAME AS RPT. ☐ DTIC USERS ☐	21. ABSTRACT SECURITY CLASSIFICATION UNCLASSIFIED	
22a. NAME OF RESPONSIBLE INDIVIDUAL Dr. Yung Kee Yeo	22b. TELEPHONE NUMBER (Include Area Code) (513)255-4498	22c. OFFICE SYMBOL AFIT/ENP

DD FORM 1473, 83 APR   EDITION OF 1 JAN 73 IS OBSOLETE.

measured profile from a real profile.

The method for correction is the following. First, assume a real profile is known. Calculate the depletion width for this profile. From these depletion widths and the Pearson type-IV fit to the original measured data construct a new assumed real profile. Repeat this procedure self-consistently until convergence of the assumed real data to a stable profile. This is the true profile. Convergence is expected in approximately 7 iterations.

END

FILMED

5-86

DTIC